

Effects of $\Lambda\Lambda$ - ΞN mixing in the decay of $S = -2$ hypernuclei

Jordi Maneu, Assumpta Parreño, and Àngels Ramos

Departament de Física Quàntica i Astrofísica and Institut de Ciències del Cosmos, Universitat de Barcelona, Martí i Franquès, 1, E-08028 Barcelona, Spain



(Received 19 June 2018; published 28 August 2018)

The nonmesonic weak decay of the doubly strange hypernucleus ${}_{\Lambda\Lambda}^6\text{He}$ is studied within a model that considers the exchange of pseudoscalar and vector mesons. Special attention is paid to quantifying the strong interaction effects, focusing on the interaction among the two Λ hyperons that induces novel weak transitions, whereby $\Lambda\Lambda$, ΞN , and $\Sigma\Sigma$ states decay into a hyperon-nucleon pair. The initial strangeness -2 wave function is obtained from the solution of a G -matrix equation with the input of realistic strong baryon-baryon potentials, while the final hyperon-nucleon wave functions are derived analogously from a microscopic T -matrix calculation. The new $\Lambda\Lambda \rightarrow YN$ decay rate studied in this work, $\Gamma_{\Lambda n} + \Gamma_{\Sigma^0 n} + \Gamma_{\Sigma^- p}$, represents 3–4% of the total one-baryon-induced nonmesonic decay and is remarkably affected by strong interaction effects. In particular, the relative importance of the partial decay rates encoded in the ratio $\Gamma_{\Lambda n}/(\Gamma_{\Sigma^0 n} + \Gamma_{\Sigma^- p})$ gets inverted when the mixing to ΞN states is incorporated in the initial correlated $\Lambda\Lambda$ wave function. This sensitivity can be used experimentally to learn about the strong interaction in the strangeness -2 sector.

DOI: [10.1103/PhysRevC.98.025208](https://doi.org/10.1103/PhysRevC.98.025208)

I. INTRODUCTION

Since the discovery in 1952 of the first strange fragment in emulsion chamber experiments, much effort has been invested in extending our knowledge of the nuclear chart towards the $SU(3)$ sector. Worldwide, the study of the interactions among nucleons and hyperons has been a priority in the research plans of many experimental facilities. After more than 60 years of Λ -hypernuclear studies, remarkable effort has been devoted to characterizing doubly strange systems, examples being the production of $\Lambda\Lambda$ hypernuclei and, more recently, the study of Ξ -hypernuclear spectroscopy. The most effective way of producing doubly strange hypernuclei is through the (K^-, K^+) reaction, which transfers two strangeness and charge units to the target nucleus. Employing high-intensity K^- beams of 1.8 MeV/ c and high-resolution spectrometers, the E05 experiment [1] at J-PARC plans on producing ${}_{\Xi}^{12}\text{Be}$ hypernuclei, with the goal of studying their spectroscopy, as well as obtaining information on the Ξ potential depth and the $\Xi N \rightarrow \Lambda\Lambda$ conversion width. The E07 experiment [2] at J-PARC aims to produce double- Λ hypernuclei in emulsion, following the capture of Ξ^- hyperons at rest, with ten times more statistics than the KEK-E373 experiment [3] that led to the observation of the ${}_{\Lambda\Lambda}^6\text{He}$ hypernucleus (Nagara event) and established the mild attractive character of the $\Lambda\Lambda$ interaction. Note that a recent reanalysis [4,5] of the KEK-E373 experiment also provided direct evidence for the existence of a bound Ξ^- hypernucleus ${}_{\Xi}^{15}\text{C}$ (Kiso event), produced in the reaction $\Xi^- + {}^{14}\text{N} \rightarrow {}_{\Xi}^{15}\text{C} \rightarrow {}_{\Lambda}^{10}\text{Be} + {}_{\Lambda}^5\text{He}$.

Once produced, these strange baryons are unstable with respect to the weak interaction and decay through reactions that do not conserve parity, strangeness, or isospin. Being that the Λ hyperon is the lightest hyperon, its weak decay modes in free space, $\Lambda \rightarrow N\pi$, have been measured with good

precision. These mesonic decay channels show, for instance, that transitions that involve a change in isospin of $3/2$ are suppressed with respect to those involving a $1/2$ variation, a phenomenon known as the $\Delta I = 1/2$ rule. Although its origin is not well understood yet, its validity is assumed in most of the theoretical studies of weak processes involving hadrons. In a hypernucleus, the Λ hyperon is embedded in the nuclear medium, and its mesonic decay mode becomes Pauli blocked as the number of baryons increases, because the emerging nucleon tries to access momentum states that are essentially occupied by the surrounding nucleons. Under such circumstances, new decay mechanisms involving more baryons and with no mesons in the final state start playing an important role. The dominant decay mode for single- Λ hypernuclei with $A > 5$ is through the two-body process $\Lambda N \rightarrow NN$, whereas for double- Λ hypernuclei additional hyperon-induced mechanisms, $\Lambda\Lambda \rightarrow \Lambda n$, $\Lambda\Lambda \rightarrow \Sigma^- p$, and $\Lambda\Lambda \rightarrow \Sigma^0 n$ (globally referred to as $\Lambda\Lambda \rightarrow YN$ henceforth), become possible.

Therefore, hypernuclei constitute not only a convenient framework to obtain information on the strong baryon-baryon interaction but also, through their decay, and using the change of strangeness as a signature, a suitable scenario to access both the parity-conserving (PC) and the parity-violating (PV) components of the four-fermion weak interaction. The large amount of experimental and theoretical work in the strangeness -1 sector (see the reviews [6–8]) has led to a consistent interpretation of the experimental data [9–15], which includes not only lifetimes but also partial decay widths and asymmetries in the angular distribution of the emitted particles. Crucial elements for this success have been the inclusion of a scalar-isoscalar component [16–19] in the weak decay mechanism or the consideration of medium effects [20–25] in the decay observables, through the incorporation of

multiabsorption processes and final-state interactions in the data analysis, among others. Little is known, comparatively, about the double-strangeness systems, due to the small yields for binding two Λ particles after Ξ^- capture and the ambiguities in interpreting events owing to the formation of particle-stable excited species. However, this situation might change with the planned experiments at J-PARC, which will have much higher statistics.

Although the new hyperon-induced decay mechanisms provide novel information to constrain the theoretical models, only a limited number of theoretical groups have calculated decay rates for double- Λ hypernuclei [26–28]. With the present work we quantify, for the first time, the contribution to the decay of the ${}_{\Lambda\Lambda}^6\text{He}$ hypernucleus of the new decay modes that emerge when the strong interaction is carefully taken into account. Specifically, the weak decay process may occur from a $\Lambda\Lambda$, ΞN , or $\Sigma\Sigma$ state, which can be excited via the strong interaction from the initial $\Lambda\Lambda$ pair. The strong interaction also determines the final YN wave-function component, which may have transitioned from either a ΛN or a ΣN intermediate state.

For the weak transition we employ a meson-exchange model built upon the exchange of mesons belonging to the ground state of pseudoscalar and vector octets, thoroughly employed for single- Λ hypernuclei, and extended to the decay of double- Λ hypernuclei in Ref. [26]. The tree-level values for the baryon-baryon-meson coupling constants are derived using SU(3) symmetry for pseudoscalar mesons and hidden local symmetry for vector mesons. In the computation of the decay rate, the effects of the strong interaction on the initial state are introduced through the solution of a G -matrix equation, with the input of realistic baryon-baryon potentials [29], while the final hyperon-nucleon wave functions are obtained in an analogous way, by solving the corresponding T -matrix equation. The essential development with respect to previous calculations [26] is the consideration of the weak decay processes from those intermediate states that can be coupled to the initial $\Lambda\Lambda$ wave function. This requires the use of G -matrix wave functions for the coupled transitions $\Lambda\Lambda$ - $\Lambda\Lambda$ and $\Lambda\Lambda$ - ΞN . We show that the $\Lambda\Lambda$ - $\Sigma\Sigma$ component is very small and therefore it is neglected in our calculations. Furthermore, the transition potential for the weak ΞN - YN amplitude, where Y can be either the Λ or the Σ baryon, requires the derivation of novel decay constants. These two new ingredients have allowed us to obtain an update on the decay rate for the $(\Lambda\Lambda$ - $\Lambda\Lambda) \rightarrow (YN$ - $Y'N')$ channel as well as new results for the $(\Lambda\Lambda$ - $\Xi N) \rightarrow (YN$ - $Y'N')$ channel, where Y' follows the same criteria as Y .

The manuscript is organized as follows. In Sec. II we present the formalism used to decompose the hypernuclear decay amplitude for ${}_{\Lambda\Lambda}^6\text{He}$ in terms of two-body $\Lambda\Lambda \rightarrow YN$ amplitudes. The details on how the final YN and initial $\Lambda\Lambda$ wave functions are built are given in Sec. III, where results for the different components of the initial-state wave function are explicitly shown. The derivation of the isospin structure of the nonrelativistic one-meson-exchange potential employed in the present work is described in Sec. IV, while the description of the Lagrangians and the methodology for obtaining the coupling constants at the strong and weak vertices is relegated

to the Appendix. Our results are shown in Sec. V and some concluding remarks are given in Sec. VI.

II. HYPERNUCLEAR DECAY RATE

The nonmesonic decay rate of a hypernucleus is given by

$$\Gamma_{\text{nm}} = \int \frac{d^3k_1}{(2\pi)^3} \int \frac{d^3k_2}{(2\pi)^3} \sum_{\substack{M_I\{R\} \\ \{1\}\{2\}}} (2\pi) \times \delta(M_H - E_R - E_1 - E_2) \frac{1}{2J+1} |\mathcal{M}_{fi}|^2, \quad (1)$$

where M_H , E_R , E_1 , and E_2 correspond to the mass of the hypernucleus, the energy of the $(A-2)$ -particle system, and the total asymptotic energies of the emitted baryons, respectively. The integration variables \vec{k}_1 and \vec{k}_2 stand for the momenta of the two particles in the final state. The momentum-conserving δ function has been used to integrate over the momentum of the residual nucleus. The sum, together with the factor $1/(2J+1)$, indicates an average over the initial hypernucleus spin projections, M_I , and a sum over all quantum numbers of the residual $(A-2)$ -particle system, $\{R\}$, as well as the spin and isospin projection of the emitted final particles, $\{1\}$ and $\{2\}$ (henceforth referred to as $\overline{\Sigma}$). \mathcal{M}_{fi} stands for the transition amplitude from an initial hypernuclear state $({}_{\Lambda\Lambda}^6\text{He}$ in the present study) to a final state composed of a residual nuclear core plus two outgoing baryons. When a transformation to the total momentum, $\vec{P} = \vec{k}_1 + \vec{k}_2$, and the relative momentum, $\vec{k} = (\vec{k}_1 - \vec{k}_2)/2$, of the two outgoing particles is performed, the expression for Γ_{nm} becomes

$$\Gamma_{\text{nm}} = \int \frac{d^3P}{(2\pi)^3} \int \frac{d^3k}{(2\pi)^3} \overline{\Sigma} (2\pi) \times \delta(M_H - E_R - E_1 - E_2) |\mathcal{M}_{fi}|^2. \quad (2)$$

We write the hypernuclear transition amplitude \mathcal{M}_{fi} in terms of elementary two-body transitions, $B_1 B_2 \rightarrow B'_1 B'_2$, by using a shell-model framework where Λ hyperons and nucleons are described, in a first approximation, by harmonic oscillator single-particle orbitals. The oscillator parameter of the Λ particle ($b_\Lambda = 1.6$ fm) has been chosen to simulate the uncorrelated $\Lambda\Lambda$ probability shown in the variational approach of Ref. [30], where a fit to the binding energies of a few double- Λ hypernuclei was performed. Because a proper few-body calculation of the ${}_{\Lambda\Lambda}^6\text{He}$ wave function with coupled-channel potentials is a prohibitive task, we have adopted a pragmatic solution to incorporate the effect of the $\Lambda\Lambda$ correlations, which is quite realistic when the interactions are short ranged. As is explained in the next section, the uncorrelated wave function is corrected via a correlation function, which is obtained from solving the $\Lambda\Lambda$ - ΞN - $\Sigma\Sigma$ coupled-channel scattering problem in nuclear matter employing a realistic hyperon-hyperon interaction. This approximation allows us to study for the first time the contribution of the intermediate ΞN wave-function components to the weak decay of double- Λ hypernuclei. In the case of the nucleons, we adopt an oscillator parameter of $b_N = 1.4$ fm, which reproduces the ${}^4\text{He}$ charge form factor and, hence, the size of the nuclear core.

Therefore, in the case of the ${}_{\Lambda\Lambda}^6\text{He}$ hypernucleus studied here, with spin and isospin quantum numbers $J_I = M_I = 0$ and $T_I = M_{T_I} = 0$, the state is given by

$$|{}_{\Lambda\Lambda}^6\text{He}\rangle = |\Lambda\Lambda\rangle_{T=M_T=0}^{J=M=0} \otimes |{}^4\text{He}\rangle_{T_c=M_{T_c}=0}^{J_c=M_c=0}, \quad (3)$$

where antisymmetry forces the two Λ hyperons to be in a 1S_0 state, because they are assumed to be in the lowest s -shell ($1s_{1/2}$) before the decay occurs. This is so because, in general, a Λ hyperon in an excited orbital will rapidly decay into the ground state through electromagnetic or strong deexcitation processes, which are orders of magnitude faster than those mediated by the weak interaction.

The evaluation of the $\Lambda N \rightarrow NN$ transition rate requires one to decompose the nonstrange nuclear core in terms of one nucleon coupled to a three-particle system, while decoupling one of the two Λ particles, so that the initial ΛN pair can convert into a final NN pair, conveniently antisymmetrized with the residual nuclear core. The details and final expression for the hypernuclear decay amplitude in terms of two-body $\Lambda N \rightarrow NN$ transitions can be found in Ref. [26]. Here, we focus on the $\Lambda\Lambda \rightarrow YN$ decay mode, which is the one we improve with respect to earlier calculations. In this case, the Λ hyperon does not need to be decoupled from the cluster, nor does a nucleon need to be decoupled from the core. The residual four-particle system, which coincides with the ${}^4\text{He}$ nucleus, contains no strangeness, while the final two-particle state contains one hyperon than can be a Λ ($|Yt_Y\rangle = |00\rangle$), a Σ^- ($|Yt_Y\rangle = |1-1\rangle$) or a Σ^0 ($|Yt_Y\rangle = |10\rangle$) hyperon. The hypernuclear amplitude associated with the $\Lambda\Lambda \rightarrow YN$ transition is then given by

$$\begin{aligned} \mathcal{M}_{\Lambda\Lambda \rightarrow YN} &= \langle \vec{k}_{NS} s_N t_N, \vec{k}_Y s_Y t_Y; {}^4\text{He} | \hat{O} | {}_{\Lambda\Lambda}^6\text{He} \rangle \left| \frac{1}{2} - \frac{1}{2} \right\rangle_{\Lambda} \\ &= \sum_{S', M'_S} \left\langle \frac{1}{2} s_N, \frac{1}{2} s_Y \left| S' M'_S \right. \right\rangle \left\langle \frac{1}{2} t_N, Y t_Y \left| T' M'_T \right. \right\rangle \\ &\quad \times \langle \vec{K} | \Psi_{\Lambda\Lambda}^{c.m.} \rangle \langle \vec{k}_Y, S' M'_S, T' M'_T | \\ &\quad \times \hat{O} | \Psi_{\Lambda\Lambda}^{\text{rel}}, S M_S, T M_T \rangle, \end{aligned} \quad (4)$$

where the initial $\Lambda\Lambda$ wave function has been written as a product of relative and center-of-mass wave functions, $\Psi_{\Lambda\Lambda}^{\text{rel}}$ and $\Psi_{\Lambda\Lambda}^{c.m.}$, respectively, and \vec{k} and \vec{K} are the relative and total momentum of the emitted YN pair. The amplitude $\langle \vec{k}, Y S' M'_S, T' M'_T | \hat{O} | \Psi_{\Lambda\Lambda}^{\text{rel}}, S M_S, T M_T \rangle$ represents the two-body transition matrix element. The spin quantum numbers of the $\Lambda\Lambda$ pair are $S = M_S = 0$, due to antisymmetrization, while its isospin quantum numbers are $T = 1/2$ and $M_T = -1/2$, which contain the coupling to the isospurion field $|\frac{1}{2} - \frac{1}{2}\rangle_{\Lambda}$ introduced to account for the $\Delta I = 1/2$ rule in the transition. The isospin quantum numbers of the emitted pair fulfill $T' = T = 1/2$ and $M'_T = M_T = -1/2$ by isospin conservation.

These two-body matrix elements are calculated using a two-body interaction potential based on a meson-exchange picture, including initial and final correlated wave functions which are derived through the resolution of the G -matrix formalism for the former and the Lippmann-Schwinger equation for the latter. Further details will be given in the following sections.

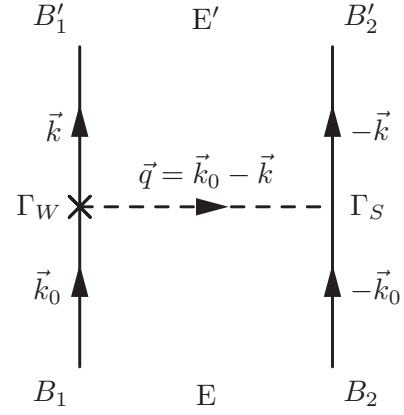


FIG. 1. Diagrammatic representation of a $B_1 B_2 \rightarrow B'_1 B'_2$ transition within a one-meson-exchange model. The cross represents an insertion of a weak vertex.

In the case of the $\Lambda\Lambda \rightarrow YN$ decay, and since the strong interaction allows for the conversion to other baryon-baryon channels, the weak interaction will take place not only from the initial $\Lambda\Lambda$ pair, but also from pairs containing other members of the baryon octet, $\Xi^- p$, $\Xi^0 n$, $\Sigma^0 \Sigma^0$ and $\Sigma^+ \Sigma^-$, which will in turn decay weakly into either Λn , $\Sigma^0 n$, or $\Sigma^- p$ states. Moreover, the strong interaction acting between the final baryons will produce additional $Y'N \rightarrow YN$ transitions, with Y', Y being Λ or Σ hyperons.

In a meson-exchange picture, every weak $B_1 B_2 \rightarrow B'_1 B'_2$ transition can be understood in terms of the exchange of mesons between the interacting particles, with masses related to the inverse of the interaction range and with quantum numbers allowed by the symmetries governing the underlying dynamics. Within this model, the transition involves a product of a strong vertex and a weak one, where the change in strangeness occurs, connected through the meson propagator (see Fig. 1).

We note that, while the calculation corresponding to the exchange of pseudoscalar mesons other than the pion requires the use of $SU(3)_f$ symmetry to obtain the baryon-baryon-meson vertices, the inclusion of vector mesons requires the generalization of the hidden local symmetry (HLS) formalism [31] to the strange strong sector and the implementation of $SU(6)_W$ for the weak vertices, as explained in the Appendix. One might also use the less model-dependent effective field theory approach to describe the four-fermion weak interaction, which would replace those vector meson exchanges by contact terms [19,32–34]. These contributions are organized as an expansion of increasing dimension (powers of some *small* ratio of physical scales), providing a more systematic and controllable framework to study the weak process. The size of the coefficients in the expansion is constrained by fitting to accurate experimental data. At present, there are no measurements for the required weak transitions in the strangeness -2 sector, and one has to rely on model determinations of the decay mechanism. In the present work, we build up a meson-exchange approach following our previous works for the weak decay of single- Λ hypernuclei and extend the decay model of Ref. [26] for $S = -2$ systems by incorporating new

TABLE I. Possible $^{2S+1}L_J$ channels involved in the weak process $\Lambda\Lambda \rightarrow B_1 B_2 \rightarrow B'_1 B'_2 \rightarrow YN$ contributing to the weak decay of ${}^6_{\Lambda\Lambda}\text{He}$, where the first and last transitions are mediated by the strong interaction.

$\Lambda\Lambda$	\rightarrow	$B_1 B_2$	\rightarrow	$B'_1 B'_2$	\rightarrow	YN
(Λ)		(\tilde{Y})		(Y')		(Y)
$^{2S+1}L_J$		$^{2\tilde{S}+1}\tilde{L}_J$		$^{2S'+1}\tilde{L}'_J$		$^{2S'+1}L'_J$
1S_0	\rightarrow	1S_0	\rightarrow	1S_0	\rightarrow	1S_0
1S_0	\rightarrow	1S_0	\rightarrow	3P_0	\rightarrow	3P_0

decay channels induced by short-range correlations in the initial state.

III. STRONG INTERACTIONS

In this section we discuss how to incorporate the strong interaction effects into the calculation of the weak decay amplitude. We employ the G -matrix formalism to obtain the correlated wave function for the initial hyperon-hyperon state, which takes into account the Pauli-blocking effects on the nucleon of the intermediate ΞN pair. For the description of the final YN system, the relevant strong interaction effects in the evaluation of decay rates are those associated with their mutual interaction, which can be addressed by solving the corresponding T -matrix equation. The propagation of these two baryons through the residual nuclear medium induces additional final-state interactions, which modify energy and angular spectra of the emitted particles. Using an intranuclear cascade code (Monte Carlo), one can then make comparisons to experimental data at the level of the detected particle spectra. Because our interest with the present calculation is to estimate decay rates, which are not affected by spectral distributions, we omit these residual final-state interaction effects and focus only on the interaction between the two weakly emitted baryons. Note that, given the angular quantum numbers of the $\Lambda\Lambda$ initial state, 1S_0 , the possible $^{2S+1}L_J$ channels involved in the process $\Lambda\Lambda \rightarrow B_1 B_2 \rightarrow B'_1 B'_2 \rightarrow YN$ are listed in Table I, where conservation of total angular momentum, as well as conservation of parity for the strong interaction transitions, has been taken into account. The symbols in parentheses denote the labels that represent the different baryon-baryon channels in the two-body states.

A. Final state

The effect of the strong interaction between the outgoing hyperon and nucleon can be accounted for by the YN wave functions. Let the Hamiltonian be $H = H_0 + V$. If we denote by Φ the plane-wave solution, $|\vec{k}Y S' M'_S\rangle$, of the Hamiltonian H_0 with energy E , i.e., $H_0\Phi = E\Phi$, then the possible solutions for Ψ are given by the Lippmann-Schwinger equation,

$$|\Psi^{(\pm)}\rangle = |\Phi\rangle + \frac{V|\Psi^{(\pm)}\rangle}{E - H_0 \pm i\epsilon}, \quad (5)$$

where the positive (negative) solution corresponds to a plane wave plus an outgoing (incoming) spherical wave at

sufficiently large distances. An alternative formulation of the Lippmann-Schwinger equation written in terms of the transition matrix T yields

$$|\Psi^{(+)}\rangle = |\Phi\rangle + \frac{T|\Phi\rangle}{E - H_0 + i\epsilon}, \quad (6)$$

$$\langle\Psi^{(-)}| = \langle\Phi| + \frac{\langle\Phi|T}{E - H_0 - i\epsilon}, \quad (7)$$

where the T operator fulfills

$$T = V + V \frac{T}{E - H_0 + i\epsilon}. \quad (8)$$

Projecting into coordinate space and inserting a complete set of states on the right-hand side in Eq. (7) we find

$$\begin{aligned} &\langle\Psi_k^{(-)}|Y S' M'_S|\vec{r}\rangle \\ &= \langle\vec{k}Y S' M'_S|\vec{r}\rangle + \sum_{\tilde{S}'\tilde{M}'_S} \sum_{Y'} \int d^3k' \\ &\quad \times \frac{\langle\vec{k}Y S' M'_S|T|\vec{k}'Y'\tilde{S}'\tilde{M}'_S\rangle \langle\vec{k}'Y'\tilde{S}'\tilde{M}'_S|\vec{r}\rangle}{E - H_0 - i\epsilon}. \end{aligned} \quad (9)$$

We perform a partial-wave decomposition in the coupled $(LS)J$ representation of the wave functions $\langle\Psi_k^{(-)}|Y S' M'_S|\vec{r}\rangle$ and $\langle\vec{k}Y S' M'_S|\vec{r}\rangle$, the latter being the adjoint of the free plane wave, $e^{-i\vec{k}\vec{r}}\langle Y S' M'_S|$, and obtain

$$\begin{aligned} &\Psi_{\vec{k}Y}^{(-)*}(\vec{r})\chi_{M'_S}^{S'} \\ &= 4\pi \sum_{JM} \sum_{L'M'_L\tilde{L}'\tilde{S}'} \sum_{Y'} (-i)^{\tilde{L}'} \Psi_{Y'L'S',Y'\tilde{L}'\tilde{S}'}^{(-)*J}(k, r) Y_{L'M'_L}(\hat{k}) \\ &\quad \times \langle L'M'_L S' M'_S | JM \rangle \mathcal{J}_{\tilde{L}'\tilde{S}'}^{\dagger JM}(\hat{r}), \end{aligned} \quad (10)$$

where the generalized spherical harmonic \mathcal{J}^\dagger is defined as

$$\mathcal{J}_{\tilde{L}'\tilde{S}'}^{\dagger JM}(\hat{r}) = \sum_{\tilde{M}'_L\tilde{M}'_S} \langle \tilde{L}'\tilde{M}'_L \tilde{S}'\tilde{M}'_S | JM \rangle Y_{\tilde{L}'\tilde{M}'_L}^*(\hat{r}). \quad (11)$$

The partial-wave decomposition for the free plane wave may be obtained by replacing $\Psi_{Y'L'S',Y'\tilde{L}'\tilde{S}'}^{(-)*J}(k, r)$ with $j_{L'}(kr)\delta_{Y'Y}\delta_{\tilde{L}'L'}\delta_{\tilde{S}'S'}$ in Eq. (10), where $j_{L'}(kr)$ is the spherical Bessel wave function.

For the T -matrix elements one can write

$$\begin{aligned} &\langle\vec{k}Y S' M'_S|T|\vec{k}'Y'\tilde{S}'\tilde{M}'_S\rangle \\ &= \sum_{JM} \sum_{L'M'_L} \sum_{\tilde{L}'\tilde{M}'_L} Y_{L'M'_L}(\hat{k}) Y_{\tilde{L}'\tilde{M}'_L}^*(\hat{k}') \\ &\quad \times \langle L'M'_L S' M'_S | JM \rangle \langle \tilde{L}'\tilde{M}'_L \tilde{S}'\tilde{M}'_S | JM \rangle \\ &\quad \times \langle kY(L'S')JM|T|k'Y'(\tilde{L}'\tilde{S}')JM\rangle. \end{aligned} \quad (12)$$

Inserting the previous equation, together with the partial-wave decomposition of the wave functions in Eq. (9), one obtains the equation that determines the partial-wave components of

the correlated wave function:

$$\begin{aligned} \Psi_{Y L' S', Y' \tilde{L}' \tilde{S}'}^{(-)*J}(k, r) &= j_L(kr) \delta_{Y' Y} \delta_{\tilde{L}' L'} \delta_{\tilde{S}' S'} + \int k'^2 dk' \\ &\times \frac{\langle kY(L'S')JM|T|k'Y'(\tilde{L}'\tilde{S}')JM\rangle j_{\tilde{L}'}(k'r)}{E(k) - E(k') + i\epsilon}, \end{aligned} \quad (13)$$

where the partial-wave T -matrix elements fulfill the integral equation:

$$\begin{aligned} \langle kY(L'S')JM|T|k'Y'(\tilde{L}'\tilde{S}')JM\rangle &= \langle kY(L'S')JM|V|k'Y'(\tilde{L}'\tilde{S}')JM\rangle \\ &+ \sum_{L''S''Y''} \int k''^2 dk'' \langle kY(L'S')JM|V|k''Y''(L''S'')JM\rangle \\ &\times \frac{\langle k''Y''(L''S'')JM|T|k'Y'(\tilde{L}'\tilde{S}')JM\rangle}{E(k) - E(k'') + i\epsilon}. \end{aligned} \quad (14)$$

Note that, because the $\Lambda\Lambda$ pair is in a 1S_0 state, conservation of angular momentum and parity prevents a change of the spin and orbital angular momentum quantum numbers between the pre- and post-strong transition states, as seen in Table I. Consequently, the above equations could be simplified by applying $L'' = \tilde{L}' = L'$, $\tilde{M}_{L'} = M_{L'}$, $S'' = \tilde{S}' = S'$, and $\tilde{M}_{S'} = M_{S'}$.

B. Initial state

For the initial-state interactions a framework similar to that of the Lippmann-Schwinger equation is applied, but considering the fact that the interacting particles feel the presence of the medium where they are embedded. This is known as the Brueckner-Goldstone theory, which considers the interactions of a pair of particles within the Fermi sea, with the collisions fulfilling the requirements of the Pauli principle. We solve the problem in infinite nuclear matter and the obtained results are applied to the finite hypernuclear problem that we are dealing with.

Working within the $(\frac{1}{2})^+$ baryon octet, the strange $\Lambda\Lambda$, ΞN , and $\Sigma\Sigma$ pairs can couple through the strong interaction to the initial $\Lambda\Lambda$ state. The correlated state $|\Psi\rangle$ is defined through $G|\Psi\rangle = V|\Phi\rangle$, where $|\Phi\rangle$ is the free-particle state, and G is given in terms of the bare baryon-baryon potential V by

$$G = V + V \frac{Q}{E - H_0 + i\epsilon} G. \quad (15)$$

This is an integral equation, where Q corresponds to the Pauli-blocking operator, which restricts the summation to unoccupied states above the Fermi level, and E is the energy of the interacting two-body system. The correlated state can therefore be written as

$$|\Psi\rangle = |\Phi\rangle + \frac{Q}{E - H_0 + i\epsilon} G|\Phi\rangle. \quad (16)$$

Working in the coupled $(LS)J$ representation, we find

$$\begin{aligned} \Psi_{\tilde{Y}\tilde{L}\tilde{S},\Lambda LS}^J(k, r) &= j_L(kr) \delta_{\Lambda\tilde{Y}} \delta_{L\tilde{L}} \delta_{S\tilde{S}} + \int k'^2 dk' \\ &\times \frac{\langle k'\tilde{Y}(\tilde{L}\tilde{S})JM|G|kY\Lambda(LS)JM\rangle \bar{Q}(k') j_{\tilde{L}}(k'r)}{E(k) - E(k') + i\epsilon}, \end{aligned} \quad (17)$$

where \bar{Q} stands for the angle-averaged Pauli operator and the partial-wave G -matrix elements fulfill the integral equation:

$$\begin{aligned} \langle k'\tilde{Y}(\tilde{L}\tilde{S})JM|G|k\Lambda(LS)JM\rangle &= \langle k'\tilde{Y}(\tilde{L}\tilde{S})JM|V|k\Lambda(LS)JM\rangle \\ &+ \sum_{L''S''Y''} \int k''^2 dk'' \langle k'\tilde{Y}(\tilde{L}\tilde{S})JM|V|k''Y''(L''S'')JM\rangle \\ &\times \frac{\bar{Q}(k'') \langle k''Y''(L''S'')JM|G|k\Lambda(LS)JM\rangle}{E(k) - E(k'') + i\epsilon}. \end{aligned} \quad (18)$$

As before, conservation of angular momentum and parity, together with the fact that the initial $\Lambda\Lambda$ is in a 1S_0 state, simplifies the above equations considerably, as the only permitted transition is $^1S_0 \rightarrow ^1S_0$.

To obtain the wave functions in a finite hypernucleus a correlation function is defined:

$$f_{\Lambda LS}^J(r) \equiv \frac{\Psi_{\Lambda LS, \Lambda LS}^J(k^*, r)}{j_L(k^*r)}. \quad (19)$$

This function ascribes the correlated wave function in nuclear matter, $\Psi_{\Lambda LS, \Lambda LS}^J(k, r)$, with the noninteracting one for a relative momentum k^* , taken to be 100 MeV, which is representative of the average momentum of the $\Lambda\Lambda$ pair in ${}_{\Lambda\Lambda}^6\text{He}$. The same correlation effects are assumed for finite nuclei, thus defining the diagonal terms of the relative motion wave function in a finite nucleus as

$$\Omega_{\Lambda LS}^J(r) \equiv f_{\Lambda LS}^J(r) \Phi_{NL} \left(\frac{r}{\sqrt{2}b} \right), \quad (20)$$

where $\Phi_{NL}(r/\sqrt{2}b)$ is the relative harmonic oscillator wave function of the two Λ particles.

For the nondiagonal $\Lambda LS \rightarrow \tilde{Y}\tilde{L}\tilde{S}$ components, we rescale the nuclear matter wave function $\Psi_{\tilde{Y}\tilde{L}\tilde{S}, \Lambda LS}^J$ by the same normalization factor affecting the diagonal components, namely

$$\Omega_{\tilde{Y}\tilde{L}\tilde{S}, \Lambda LS}^J(r) \equiv \frac{\Phi_{NL}(r=0)}{j_L(k^*r=0)} \Psi_{\tilde{Y}\tilde{L}\tilde{S}, \Lambda LS}^J(k^*, r), \quad (21)$$

as can be inferred upon inspecting Eqs. (19) and (20).

In Fig. 2 we represent the initial $\Lambda\Lambda$ wave function for $N = 1$ and $L = 0$ as a function of the relative distance between the two Λ particles. The black solid line displays the uncorrelated harmonic oscillator wave function, while the green dashed line displays the correlated wave function for the dominant diagonal $\Lambda\Lambda$ - $\Lambda\Lambda$ component. The red dot-dot-dashed and the blue dotted lines represent, respectively, the $\Lambda\Lambda$ - $\Sigma\Sigma$ and the $\Lambda\Lambda$ - ΞN components. It is clear that the dominant contribution to the $\Lambda\Lambda \rightarrow YN$ decay mode of ${}_{\Lambda\Lambda}^6\text{He}$ will come from the diagonal $\Lambda\Lambda$ - $\Lambda\Lambda$ component of the wave function, which at large distances behaves as an uncorrelated harmonic

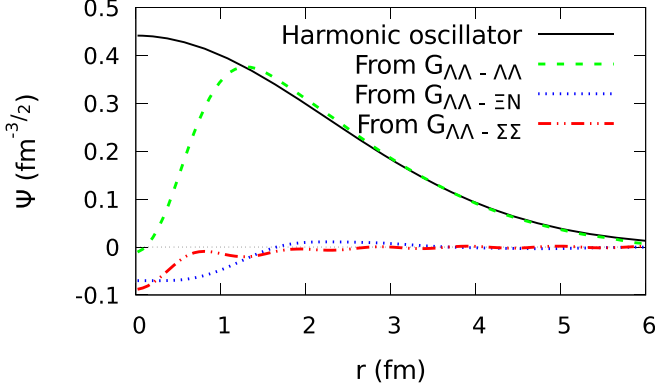


FIG. 2. Different components of the relative $\Lambda\Lambda$ radial wave function corresponding to the 1S_0 channel and for a value of the relative momentum of 100 MeV.

oscillator while at short distances its strength gets reduced due to the short-distance repulsive behavior of the strangeness $S = -2$ baryon-baryon NSC97f interaction employed [29]. With regard to the nondiagonal components of the wave function one can see that, despite having a comparable size at the origin, the strength of the $\Lambda\Lambda$ - $\Sigma\Sigma$ term is essentially located at distances under 0.5 fm, which will be strongly suppressed by the r^2 factor in the integrand of the two-body matrix element. On the other hand, the $\Lambda\Lambda$ - ΞN component is still sizable around 1 fm and it is expected to contribute non-negligibly to the $\Lambda\Lambda \rightarrow YN$ decay mode of ${}_{\Lambda\Lambda}^6\text{He}$. We show that, even if non-negligible, this nondiagonal component gives only a 10% correction to the diagonal contribution, a finding that justifies that in this work we disregard the contributions to the decay coming from the $\Lambda\Lambda$ - $\Sigma\Sigma$ component of the initial $\Lambda\Lambda$ wave function.

IV. ONE-MESON-EXCHANGE POTENTIAL

The evaluation of the two-body transition matrix elements of Eq. (4) requires the knowledge of the operator that triggers the weak $\Delta S = -1$ transition from an initial baryon pair to a final one. In the meson-exchange description employed here these transitions are assumed to proceed via exchange of virtual mesons belonging to the pseudoscalar and vector meson octets. The corresponding transition potential is obtained from the amplitude displayed in Fig. 1, which is written as

$$\mathcal{M} = \int d^4x d^4y \bar{\Psi}_1(x) \Gamma_1 \Psi_1(x) \Delta_\phi(x-y) \bar{\Psi}_2(y) \Gamma_2 \Psi_2(y), \quad (22)$$

with Γ_i being the Dirac operators characteristic of the baryon-baryon-meson vertices and $\Delta_\phi(x-y)$ the meson (ϕ) propagator:

$$\Delta_\phi(x-y) = \int \frac{d^4q}{(2\pi)^4} \frac{e^{iq(x-y)}}{(q^0)^2 - \vec{q}^2 - m_\phi^2}. \quad (23)$$

Combining the above two expressions, performing a change to center-of-mass (c.m.) and relative variables, and integrating over the c.m., time, and energy variables, one obtains the amplitude in terms of the vertices that come from the matrix elements between fields, $\bar{\Psi}(x) \Gamma \Psi(x)$. In Table II we show the

TABLE II. Pseudoscalar (PS) and vector (V) vertices entering Eq. (22) (in units of $G_F m_\pi^2 = 2.21 \times 10^{-7}$).

	PS	V
Strong	$ig\gamma_5$	$[g^V \gamma^\mu + i \frac{g^T}{2M} \sigma^{\mu\nu} q_\nu]$
Weak	$i(A + B\gamma_5)$	$[\alpha\gamma^\mu - \beta i \frac{\sigma^{\mu\nu} q_\nu}{2M} + \epsilon\gamma^\mu \gamma_5]$

strong and weak Γ operators for pseudoscalar (PS) and vector (V) mesons. The constants A , B , α , β , and ϵ correspond to the weak couplings, while g (g^V , g^T) represents the strong (vector, tensor) one.

We take the nonrelativistic reduction of this transition amplitude and the static $q^0 = 0$ limit, allowing us to identify $\mathcal{M}(\vec{q})$ with $V(\vec{q})$, which is the Fourier transform of the transition potential in coordinate space. As we detail below, the general structure of this potential for pseudoscalar meson exchanges reads

$$V^\phi(\vec{q}) = \sum_k \left(A_k^{Y,\phi} + \frac{B_k^{Y,\phi}}{2M} \vec{\sigma}_1 \vec{q} \right) \frac{\vec{\sigma}_2 \vec{q}}{\vec{q}^2 + m_\phi^2} \hat{O}_k^Y, \quad (24)$$

where \bar{M} is the average mass of the baryons involved in the weak vertex, m_ϕ is the mass of the exchanged meson, and the index k in the sum runs over the different isospin structures associated with each type of meson. Similarly, the potential for vector meson exchanges reads

$$V^v(\vec{q}) = \sum_k \left(i \frac{A_k^{Y,v}}{2M} (\vec{\sigma}_1 \times \vec{\sigma}_2) \vec{q} + B_k^{Y,v} + \frac{C_k^{Y,v}}{4M\bar{M}} (\vec{\sigma}_1 \times \vec{q})(\vec{\sigma}_2 \times \vec{q}) \right) \frac{1}{\vec{q}^2 + m_v^2} \hat{O}_k^Y. \quad (25)$$

The explicit expressions for the A , B , and C constants, in terms of strong and weak coupling constants, is given at the end of this section.

To build the isospin operators \hat{O}_k^Y one needs to know the isospin nature of the meson being exchanged (isoscalar for η and ω , isodoublet for K and K^* , and isovector for π and ρ) and the specific baryons involved in the two-body weak transition. Note that the $\Delta I = 1/2$ rule is implemented through the insertion of an isospurion, $|\frac{1}{2}, -\frac{1}{2}\rangle$, in the initial state. We focus on developing the isospin structure for the transitions $\Xi N \rightarrow YN$, with $Y = \Lambda$ and Σ , which are the new contributions considered in the present work. Attending only to the isospin quantum numbers, the general structure of the $\Xi N \rightarrow YN$ matrix element is

$$\begin{aligned} & g_1^{Y,\phi} \langle Y t_Y, \frac{1}{2} t_{Nf} | \hat{O}_1^Y | 0 t_\Xi - \frac{1}{2}, \frac{1}{2} t_{Ni} \rangle \\ & \times \langle 0 t_\Xi - \frac{1}{2} | \frac{1}{2} t_\Xi, \frac{1}{2} - \frac{1}{2} \rangle \\ & + g_2^{Y,\phi} \langle Y t_Y, \frac{1}{2} t_{Nf} | \hat{O}_2^Y | 1 t_\Xi - \frac{1}{2}, \frac{1}{2} t_{Ni} \rangle \\ & \times \langle 1 t_\Xi - \frac{1}{2} | \frac{1}{2} t_\Xi, \frac{1}{2} - \frac{1}{2} \rangle \\ & + g_3^{Y,\phi} \langle Y t_Y, \frac{1}{2} t_{Nf} | \hat{O}_3^Y | 1 t_\Xi - \frac{1}{2}, \frac{1}{2} t_{Ni} \rangle \\ & \times \langle 1 t_\Xi - \frac{1}{2} | \frac{1}{2} t_\Xi, \frac{1}{2} - \frac{1}{2} \rangle. \end{aligned} \quad (26)$$

where the isospurion has been coupled to the isospin $\frac{1}{2}$ of the Ξ giving states with isospins $I = 0$ and $I = 1$, which in turn couple to the initial nucleon isospins ($t_{Ni} = \frac{1}{2}$ for a p and $-\frac{1}{2}$ for a n) to give the final YN state.

We first examine those cases where the final state is of the ΛN type, i.e., $|Yt_Y\rangle = |00\rangle$. The possible isospin operators can be argued to be

$$\widehat{O}_1^\Lambda \equiv \mathbb{I}_1 \otimes \mathbb{I}_2, \quad (27)$$

$$\widehat{O}_2^\Lambda \equiv \bar{\mathbb{T}}_{01} \otimes \vec{\tau}_2, \quad (28)$$

$$\widehat{O}_3^\Lambda \equiv 0, \quad (29)$$

where $\vec{\tau}$ stands for the Pauli matrices and $\bar{\mathbb{T}}_{01}$ is an operator that allows the transition from an $I = 1$ state to an $I = 0$ one. Their spherical coordinates have the following matrix elements:

$$\langle 00|\bar{\mathbb{T}}_{01}^k|1m\rangle = (-1)^k \langle 00, 1-k|1m\rangle = (-1)^k \delta_{m,-k}. \quad (30)$$

We note that, in the case of a ΛN final state, we have set the \widehat{O}_3^Λ operator to zero to account for the fact that there is only one possible scalar operator (\widehat{O}_2^Λ) connecting the initial $|1 t_\Xi - \frac{1}{2}, \frac{1}{2} t_{Ni}\rangle$ pair with the final $(00, \frac{1}{2} t_{Nf})$ one. In the case of a ΣN final state, we have $|Yt_Y\rangle = |1t_Y\rangle$ and the corresponding appropriate set of operators is

$$\widehat{O}_1^\Sigma \equiv \bar{\mathbb{T}}_{10} \otimes \vec{\tau}_2, \quad (31)$$

$$\widehat{O}_2^\Sigma \equiv \mathbb{I}_1 \otimes \mathbb{I}_2, \quad (32)$$

$$\widehat{O}_3^\Sigma \equiv \bar{\mathbb{T}}_{11} \otimes \vec{\tau}_2, \quad (33)$$

where $\bar{\mathbb{T}}_{10}$ mediates transitions from isospin 0 to isospin 1, with matrix elements

$$\langle 1m|\bar{\mathbb{T}}_{10}^k|00\rangle = \delta_{m,k}, \quad (34)$$

as can be inferred by taking the adjoint in Eq. (30). Likewise $\bar{\mathbb{T}}_{11}$ induces transitions from an initial $I = 1$ state to a final $I = 1$ one. Its matrix elements are given by

$$\langle 1m'|\bar{\mathbb{T}}_{11}^k|1m\rangle = \sqrt{2}\langle 1m'|1m1k\rangle. \quad (35)$$

In the following, we write the isospin coefficients $g_i^{Y,\phi}$ ($i = 1, 2, 3$) in terms of the weak and strong coupling constants characteristic of the meson exchanged in either the $\Xi N \rightarrow \Lambda N$ or the $\Xi N \rightarrow \Sigma N$ process. The explicit expressions for the weak and strong coupling constants can be found in the Appendix.

In the case of the isoscalar mesons (η or ω) only the $\mathbb{I}_1 \otimes \mathbb{I}_2$ operator contributes to the transition. Therefore, for ΛN final states, the transition will match the following structure:

$$g_1^{\Lambda,\eta} \langle \frac{1}{2} t_{Nf} | \frac{1}{2} t_{Ni} \rangle \langle 0 t_\Xi - \frac{1}{2} | \frac{1}{2} t_\Xi, \frac{1}{2} - \frac{1}{2} \rangle. \quad (36)$$

The Clebsch-Gordan coefficient will only be nonzero when the initial state contains a Ξ^0 hyperon. By matching the former expression with that for the $\Xi^0 n \rightarrow \Lambda n$ transition, one obtains the corresponding relation between the isospin coupling and the product of weak and strong coupling constants. Thus, one has

$$g_1^{\Lambda,\eta} = \sqrt{2} g_{\Xi^0\Lambda\eta}^W g_{\Sigma N\eta}^S, \quad (37)$$

$$g_2^{\Lambda,\eta} = 0, \quad (38)$$

$$g_3^{\Lambda,\eta} = 0, \quad (39)$$

and similarly for the ω meson.

Considering now the case of ΣN final states, only the O_2^Σ operator can act in isoscalar meson exchange. Hence, following similar steps as in the previous case but for the $\Xi^0 n \rightarrow \Sigma^0 n$ transition, we find

$$g_1^{\Sigma,\eta} = 0, \quad (40)$$

$$g_2^{\Sigma,\eta} = \sqrt{2} g_{\Xi^0\Sigma^0\eta}^W g_{\Sigma N\eta}^S, \quad (41)$$

$$g_3^{\Sigma,\eta} = 0. \quad (42)$$

Let us now turn to the isovector (π or ρ) mesons. For ΛN final states the first isospin structure does not contribute because the isovector meson cannot connect an isospin 0 initial state with the final Λ hyperon at the weak vertex. The combined analysis of the $\Xi^0 p \rightarrow \Lambda p$, $\Xi^0 n \rightarrow \Lambda n$, and $\Xi^- p \rightarrow \Lambda n$ amplitudes therefore determines

$$g_1^{\Lambda,\pi} = 0, \quad (43)$$

$$g_2^{\Lambda,\pi} = -\frac{1}{\sqrt{2}} g_{\Xi^- \Lambda \pi^-}^W g_{n p \pi^-}^S = -g_{\Xi^- \Lambda \pi^-}^W g_{\Sigma N \pi}^S, \quad (44)$$

$$g_3^{\Lambda,\pi} = 0, \quad (45)$$

where the generic strong coupling $g_{\Sigma N \pi}^S = g_{pp\pi^0}^S = -g_{nn\pi^0}^S = g_{np\pi^-}^S/\sqrt{2}$ has been employed in the last two terms. Similarly, for the ΣN final states one finds

$$g_1^{\Sigma,\pi} = \sqrt{2} g_{\Xi^0\Sigma^0\pi^0}^W g_{\Sigma N\pi}^S, \quad (46)$$

$$g_2^{\Sigma,\pi} = 0, \quad (47)$$

$$g_3^{\Sigma,\pi} = g_{\Xi^- \Sigma^- \pi^0}^W g_{\Sigma N\pi}^S. \quad (48)$$

Finally, the case of the isodoublet (K or K^*) mesons involves the exchange of an isospin $\frac{1}{2}$ particle. After including the isospurion, as seen in Eq. (26), the isospin-conserving transitions are then mediated by isoscalar or isovector operators. In the case of ΛN final states, working out the $\Xi^0 p \rightarrow \Lambda p$ and $\Xi^0 n \rightarrow \Lambda n$ amplitudes (and the $\Xi^- p \rightarrow \Lambda n$ one as a consistency check), we find

$$g_1^{\Lambda,K} = \frac{1}{\sqrt{2}} g_{\Xi\Lambda K}^S (2g_{ppK^0}^W + g_{pnK^+}^W), \quad (49)$$

$$g_2^{\Lambda,K} = -\frac{1}{\sqrt{2}} g_{\Xi\Lambda K}^S g_{npK^+}^W, \quad (50)$$

$$g_3^{\Lambda,K} = 0, \quad (51)$$

written in terms of the generic strong coupling $g_{\Xi\Lambda K}^S = g_{\Xi^0\Lambda K^0}^S = g_{\Xi^- \Lambda K^+}^S$.

Other weak processes are possible in the case of K -exchange when the weak vertex is the $\Xi N K$ one. Those processes involve an interchange of particles in either the initial or the final state of the amplitude but the operators mediating the transition are the same as before. Therefore, after analyzing the $p\Xi^0 \rightarrow \Lambda p$, $n\Xi^0 \rightarrow \Lambda n$, and $p\Xi^- \rightarrow \Lambda n$ amplitudes, we find

$$\tilde{g}_1^{\Lambda,K} = -\frac{1}{\sqrt{2}} g_{\Lambda N K}^S (g_{\Xi^0 n K^0}^W - 2g_{\Xi^0 p K^+}^W), \quad (52)$$

$$\tilde{g}_2^{\Lambda,K} = \frac{1}{\sqrt{2}} g_{\Lambda N K}^S g_{\Xi^0 n K^0}^W, \quad (53)$$

$$\tilde{g}_3^{\Lambda,K} = 0, \quad (54)$$

written in terms of the generic strong coupling $g_{\Lambda N K}^S = g_{\Lambda p K^+}^S = g_{\Lambda n K^0}^S$.

For the ΣN final state, we find

$$g_1^{\Sigma, K} = -\frac{1}{\sqrt{2}} g_{\Sigma N K}^S g_{pnK^+}^W, \quad (55)$$

$$g_2^{\Sigma, K} = \frac{1}{\sqrt{2}} g_{\Sigma N K}^S (g_{pnK^+}^W + 2g_{ppK^0}^W), \quad (56)$$

$$g_3^{\Sigma, K} = \frac{1}{\sqrt{2}} g_{\Sigma N K}^S g_{pnK^+}^W, \quad (57)$$

written in terms of the generic strong coupling $g_{\Sigma N K}^S = g_{\Sigma^0 \Sigma^0 K^0}^S = -g_{\Sigma^- \Sigma^- K^0}^S / \sqrt{2} = -g_{\Sigma^- \Sigma^0 K^+}^S$.

For the processes in which the weak vertex is the $\Xi N K$ one, which involves an interchange of particles in the initial or final state, we find

$$\tilde{g}_1^{\Sigma, K} = \frac{1}{\sqrt{2}} g_{\Sigma N K}^S g_{\Xi^0 n \bar{K}^0}^W, \quad (58)$$

$$\tilde{g}_2^{\Sigma, K} = -\frac{1}{\sqrt{2}} g_{\Sigma N K}^S (g_{\Xi^0 n \bar{K}^0}^W - 2g_{\Xi^0 p K^-}^W), \quad (59)$$

$$\tilde{g}_3^{\Sigma, K} = -\frac{1}{\sqrt{2}} g_{\Sigma N K}^S g_{\Xi^0 n \bar{K}^0}^W, \quad (60)$$

written in terms of the generic strong coupling $g_{\Sigma N K}^S = g_{p \Sigma^+ K^-}^S = -g_{n \Sigma^0 \bar{K}^0}^S = g_{p \Sigma^+ \bar{K}^0}^S / \sqrt{2} = g_{n \Sigma^- K^-}^S / \sqrt{2}$.

In summary, in the expression of Eq. (24) for the potential mediated by pseudoscalar mesons, the constants $A_k^{Y, \phi}$ and $B_k^{Y, \phi}$ correspond to the $g_k^{Y, \phi}$ coefficients just derived, which contain products of weak and strong couplings. The weak coupling constants employed should be the parity-violating ones in the case of the $A_k^{Y, \phi}$ constants and the parity-conserving ones in the case of the $B_k^{Y, \phi}$ ones.

Similarly, the $A_k^{Y, v}$, $B_k^{Y, v}$, and $C_k^{Y, v}$ couplings appearing in the vector meson-exchange potential of Eq. (25) correspond to the $g_k^{Y, v}$ coefficients, but take into account the following considerations.

- (i) $A_k^{Y, v}$ contains the parity-violating weak coupling constant times the sum of both strong vector and tensor ones.
- (ii) $B_k^{Y, v}$ contains the parity-conserving weak vector coupling constant times the strong vector one.
- (iii) $C_k^{Y, v}$ contains the sum of both parity-conserving weak vector and tensor coupling constants times the sum of both strong vector and tensor ones.

The coupling constants are derived in the Appendix and their explicit values can be found in the tables listed there.

V. RESULTS

The results for the Λ -induced, $\Lambda \Lambda \rightarrow YN$, decay rates of ${}_{\Lambda\Lambda}^6\text{He}$ into different final states, containing a Λn , a $\Sigma^0 n$, or a $\Sigma^- p$ pair, are displayed in Tables III to VI. All quantities are given in units of the free space Λ -decay rate, $\Gamma_\Lambda = 3.8 \times 10^9 \text{ s}^{-1}$. Note that, by virtue of the $\Delta I = 1/2$ rule, isospin coupling

TABLE III. Individual and combined meson-exchange contributions to the nonmesonic decay rate of ${}_{\Lambda\Lambda}^6\text{He}$, when only the diagonal $\Lambda\Lambda$ - $\Lambda\Lambda$ component of the initial wave function is included and in the absence of final-state interactions. Results are given in units of $\Gamma_\Lambda = 3.8 \times 10^9 \text{ s}^{-1}$.

Meson	Λn	ΣN
π	–	1.94×10^{-2}
K	1.45×10^{-3}	2.41×10^{-3}
η	1.67×10^{-4}	–
ρ	–	2.20×10^{-3}
K^*	3.32×10^{-4}	2.73×10^{-3}
ω	3.20×10^{-4}	–
$\pi + K$	1.45×10^{-3}	2.69×10^{-2}
$\pi + K + \eta$	1.72×10^{-3}	2.69×10^{-2}
All	2.39×10^{-3}	4.22×10^{-2}

algebra relates the decay rates involving a Σ hyperon in the final state by a factor of 2. Therefore, the $\Lambda\Lambda \rightarrow \Sigma^0 n$ and $\Lambda\Lambda \rightarrow \Sigma^- p$ channels fulfill the relations $\Gamma_{\Sigma^0 n} = \Gamma_{\Sigma N}/3$ and $\Gamma_{\Sigma^- p} = 2\Gamma_{\Sigma N}/3$, respectively, where $\Gamma_{\Sigma N}$ collects the total ΣN decay rate, which is the one quoted in Tables III to VI. We also give the contribution of each individual meson separately to assess its importance in a given transition, and we add up the contribution of the lightest pseudoscalar mesons sequentially for a better interpretation of our results.

We start by presenting in Table III the contribution to the $\Lambda\Lambda \rightarrow YN$ decay coming from the diagonal $\Lambda\Lambda$ - $\Lambda\Lambda$ component of the wave function without the inclusion of final-state interactions, followed by the results of Table IV where these effects are considered. The strong coupling constants required to describe the $\Lambda\Lambda \rightarrow \Lambda\Lambda \rightarrow YN$ transition are taken from the Nijmegen soft-core NSC97f model [29], which has been proven to reproduce satisfactorily the scarce YN scattering data, as well as the structure of Λ hypernuclei and their decay properties. Consequently, the results presented in Tables III and IV are obtained following the same approach as that of Ref. [26], except for minor changes in the initial $\Lambda\Lambda$ and the final YN wave functions, which have been obtained with

TABLE IV. Individual and combined meson-exchange contributions to the nonmesonic decay rate of ${}_{\Lambda\Lambda}^6\text{He}$, when only the diagonal $\Lambda\Lambda$ - $\Lambda\Lambda$ component of the initial wave function is included and considering final-state interactions. Results are given in units of $\Gamma_\Lambda = 3.8 \times 10^9 \text{ s}^{-1}$.

Meson	Λn	ΣN
π	1.35×10^{-4}	7.15×10^{-3}
K	2.22×10^{-2}	9.69×10^{-4}
η	8.95×10^{-4}	7.67×10^{-7}
ρ	1.32×10^{-5}	2.37×10^{-6}
K^*	4.28×10^{-3}	2.35×10^{-4}
ω	4.95×10^{-5}	1.42×10^{-7}
$\pi + K$	2.17×10^{-2}	6.34×10^{-3}
$\pi + K + \eta$	1.41×10^{-2}	6.29×10^{-3}
All	3.00×10^{-2}	5.81×10^{-3}

higher precision here. Therefore, they have to be considered as benchmark results against which we can later assess the importance of the new $\Lambda\Lambda \rightarrow \Xi N \rightarrow YN$ transition explored in the present work.

Isospin conservation at the strong vertex excludes the exchange of a π or a ρ meson in the $\Lambda\Lambda \rightarrow \Lambda n$ transition presented in Table III, which ignores final strong interaction effects, and this is reflected as a null contribution to the decay rate for those mesons. Instead, we find that the dominant contribution to this decay mode is coming from K exchange, with a rate of $1.45 \times 10^{-3} \Gamma_\Lambda$, corresponding to roughly 60% of the rate obtained when all mesons are considered ($\Gamma_{\Lambda n} = 2.39 \times 10^{-3} \Gamma_\Lambda$). The remaining 40% of the $\Gamma_{\Lambda n}$ rate originates from the exchange of K^* , ω , and η mesons, with individual contributions which are 1 order of magnitude smaller than that for K exchange. Conversely, for the ΣN final states, one sees a clear dominance of the π -meson contribution, giving practically half of the total ΣN rate of $\Gamma_{\Sigma N} = 4.22 \times 10^{-2} \Gamma_\Lambda$. In this case, and also due to isospin considerations, the isoscalar η and ω mesons do not contribute, so the remaining rate is provided by the K , ρ , and K^* mesons with similar contributions and, again, 1 order of magnitude smaller. Adding the partial decay rates of the Λn , $\Sigma^0 n$, and $\Sigma^- p$ final states, one obtains a total $\Lambda\Lambda \rightarrow YN$ decay rate of $\Gamma_{YN} = 4.46 \times 10^{-2} \Gamma_\Lambda$, distributed into an almost negligible Λn contribution ($\sim 5\%$ of Γ_{YN}) in front of the ΣN one ($\sim 95\%$ of Γ_{YN}).

As mentioned before, the results of Table IV also correspond to the contributions to the rate from the diagonal $\Lambda\Lambda$ - $\Lambda\Lambda$ component of the wave function, but incorporate the effect of final-state interactions, which, as can be seen, reduce the total $\Lambda\Lambda \rightarrow YN$ decay rate by about 20% to a value $\Gamma_{YN} = 3.58 \times 10^{-2} \Gamma_\Lambda$. Of special note is the contribution of K exchange to the Λn mode, which gets enhanced by 1 order of magnitude when final-state interactions are implemented, becoming the dominant mechanism for the transition. Note also that a similar enhancement is seen for the contribution of the K^* meson, which represents the second dominant contribution, yet is 1 order of magnitude smaller than that of its pseudoscalar partner. In the case of ΣN final states, we observe that final-state interactions cause a similar reduction, of about a factor of 2.5, for the pseudoscalar π and K contributions, while the reduction is even larger for ρ and K^* vector meson exchange, giving rise to an overall decrease of the ΣN rate by almost 1 order of magnitude. Consequently, the inclusion of final-state interactions has inverted the relative importance of the decay modes, from 5% to 84% for the $\Lambda\Lambda \rightarrow \Lambda n$ channel and from 95% to 16% for the $\Lambda\Lambda \rightarrow \Sigma N$ one, increasing the value of the $\Gamma_{\Lambda n}/(\Gamma_{\Sigma^0 n} + \Gamma_{\Sigma^- p})$ ratio by more than a factor of 90, from 0.06 to 5.16. Since these decay channels could, in principle, be detected separately in experiments, this ratio could be used to learn about the weak decay mechanism in the strangeness $S = -2$ sector and the role played by the strong interaction in the decay process.

Another change associated with the effect of final-state interactions that can be inferred from Table IV is that previously excluded meson exchanges now contribute, albeit in a very moderate manner. This is the case of the π meson, for example, which now contributes to the $\Lambda\Lambda \rightarrow \Lambda n$ decay rate through

TABLE V. Individual and combined meson-exchange contributions to the nonmesonic decay rate of ${}^6_{\Lambda\Lambda}\text{He}$, considering final-state interactions and both components of the initial wave function, $\Lambda\Lambda$ - $\Lambda\Lambda$ and $\Lambda\Lambda$ - ΞN . The results, given in units of $\Gamma_\Lambda = 3.8 \times 10^9 \text{ s}^{-1}$, have been obtained using the strong NSC97f model.

Meson	Λn	ΣN
π	3.65×10^{-4}	5.85×10^{-3}
K	1.13×10^{-2}	1.37×10^{-2}
η	8.62×10^{-4}	1.41×10^{-4}
ρ	1.31×10^{-5}	1.86×10^{-6}
K^*	4.27×10^{-3}	2.31×10^{-4}
ω	4.85×10^{-5}	1.36×10^{-7}
$\pi + K$	7.87×10^{-3}	1.97×10^{-2}
$\pi + K + \eta$	3.66×10^{-3}	2.28×10^{-2}
All	1.31×10^{-2}	2.67×10^{-2}

the intermediate weak $\Lambda\Lambda \rightarrow \Sigma N$ transition followed by the $\Sigma N \rightarrow \Lambda n$ strong one.

Up to this point, our results are totally in line with those found in Ref. [26], as expected, because the only essential difference here is the use of slightly different correlated baryon-baryon wave functions. The novelty of the present paper is the consideration of the strong nondiagonal $\Lambda\Lambda$ - ΞN mixing of the $\Lambda\Lambda$ wave function. However, contrary to the previous case, the new strong coupling constants required for the description of the $\Xi N \rightarrow YN$ transition do not have an experimental support. For this reason, we compare the results obtained when these additional coupling constants are taken either from the same NSC97f model employed in the description of the diagonal $\Lambda\Lambda \rightarrow \Lambda\Lambda \rightarrow YN$ transition or from the chiral Lagrangians given in the Appendix.

When the $\Lambda\Lambda \rightarrow \Xi N \rightarrow YN$ component is added to the calculations using the strong coupling constants given by the Nijmegen soft-core NSC97f model [29], we obtain the results of Table V. We observe that the only significant effect of the $\Lambda\Lambda$ - ΞN mixing to the decay into a final Λn state comes from π and K exchanges. Their combined effect ends up decreasing the decay rate by more than a factor of 2, from $\Gamma_{\Lambda n} = 3.00 \times 10^{-2} \Gamma_\Lambda$ to $1.31 \times 10^{-2} \Gamma_\Lambda$. The ΣN decay channel experiences an increase of over a factor of 4, from $\Gamma_{\Sigma N} = 5.81 \times 10^{-3} \Gamma_\Lambda$ to $2.67 \times 10^{-2} \Gamma_\Lambda$. Altogether, the $\Lambda\Lambda$ - ΞN component of the wave function brings the value of the $\Gamma_{\Lambda n}/(\Gamma_{\Sigma^0 n} + \Gamma_{\Sigma^- p})$ ratio to 0.49, a factor 10 times smaller than that found when this mixing is neglected. Adding the Λn , $\Sigma^0 n$, and $\Sigma^- p$ partial rates, the total $\Lambda\Lambda \rightarrow YN$ decay rate amounts to $\Gamma_{YN} = 3.98 \times 10^{-2} \Gamma_\Lambda$, which represents a modest increase of around 10% over the case that ignored the $\Lambda\Lambda$ - ΞN piece in the initial wave function.

To assess the model dependence of the $\Lambda\Lambda$ - ΞN mixing to the $\Lambda\Lambda \rightarrow YN$ decay rate, we perform another calculation that keeps the experimentally constrained NSC97f coupling constants in the description of the weak $\Lambda\Lambda \rightarrow YN$ transition but employs, for the $\Xi N \rightarrow YN$ one, the decay model developed in this work, based on effective Lagrangians, which is described in the Appendix. The results of this hybrid model are presented in Table VI. We observe that the addition of the partial rates yields a total contribution from the $\Lambda\Lambda \rightarrow YN$

TABLE VI. Individual and combined meson-exchange contributions to the nonmesonic decay rate of ${}_{\Lambda\Lambda}^6\text{He}$, considering final-state interactions and both $\Lambda\Lambda - \Lambda\Lambda$ and $\Lambda\Lambda - \Xi N$ components of the initial wave function. The results, given in units of $\Gamma_{\Lambda} = 3.8 \times 10^9 \text{ s}^{-1}$, have been obtained using the hybrid model discussed in the Appendix.

Meson	Λn	ΣN
π	9.73×10^{-4}	5.87×10^{-3}
K	5.15×10^{-3}	9.54×10^{-3}
η	2.08×10^{-3}	1.77×10^{-4}
ρ	1.31×10^{-5}	1.95×10^{-6}
K^*	4.27×10^{-3}	2.32×10^{-4}
ω	4.85×10^{-5}	1.36×10^{-7}
$\pi + K$	1.86×10^{-3}	1.63×10^{-2}
$\pi + K + \eta$	3.75×10^{-4}	1.93×10^{-2}
All	2.86×10^{-3}	2.27×10^{-2}

decay mode of $\Gamma_{YN} = 2.55 \times 10^{-2} \Gamma_{\Lambda}$, which represents an overall decrease of around 30% over the rate obtained for the diagonal $\Lambda\Lambda$ channel only. Comparing the results of this hybrid model with those of Table V, obtained with the strong NSC97f coupling constants, we observe a drastic reduction of almost a factor of 5 in the Λn rate. This comes from the reduction by about a factor of 2 in the K -exchange rate, together with the enhancement of the π - and η -exchange contributions, with which the K -exchange contribution interferes destructively. The ΣN rate of the hybrid model is only 15% smaller than that of the model employing the strong NSC97f coupling constants. Within the hybrid model we can see that the interferences between the various meson-exchange contributions are such that the final decay rate for the $\Lambda\Lambda \rightarrow \Lambda n$ channel decreases a whole order of magnitude with respect to the case that ignores the $\Lambda\Lambda$ - ΞN mixing, from $\Gamma_{\Lambda n} = 3.00 \times 10^{-2} \Gamma_{\Lambda}$ to $2.86 \times 10^{-3} \Gamma_{\Lambda}$. This is partially compensated by a major increase in the ΣN decay, from $\Gamma_{\Sigma N} = 5.81 \times 10^{-3} \Gamma_{\Lambda}$ to $2.27 \times 10^{-2} \Gamma_{\Lambda}$. Altogether, the $\Lambda\Lambda$ - ΞN component of the wave function reduces the value of the $\Gamma_{\Lambda n}/(\Gamma_{\Sigma^0 n} + \Gamma_{\Sigma^- p})$ ratio obtained with only the diagonal $\Lambda\Lambda \rightarrow \Lambda\Lambda$ component by a factor of 40, down to a value of 0.13, further highlighting the effect of the $\Lambda\Lambda$ - ΞN mixing in inverting the dominance with regards to the Λn and ΣN decay modes.

The effect of the $\Lambda\Lambda$ - ΞN mixing to the $\Lambda\Lambda \rightarrow YN$ decay modes of ${}_{\Lambda\Lambda}^6\text{He}$ is summarized in Table VII, where we

TABLE VII. Total $\Lambda\Lambda \rightarrow YN$ contribution to the weak decay rate of ${}_{\Lambda\Lambda}^6\text{He}$ and the ratio $\Gamma_{\Lambda n}/(\Gamma_{\Sigma^0 n} + \Gamma_{\Sigma^- p})$, considering only the diagonal component of the $\Lambda\Lambda$ wave function and including also the $\Lambda\Lambda$ - ΞN mixing employing two different models. The rates are given units of $\Gamma_{\Lambda} = 3.8 \times 10^9 \text{ s}^{-1}$.

Model	Γ_{YN}	$\Gamma_{\Lambda n}/\Gamma_{\Sigma N}$
$\Lambda\Lambda \rightarrow \Lambda\Lambda \rightarrow YN$	3.58×10^{-2}	5.2
$\Lambda\Lambda \rightarrow \Lambda\Lambda \rightarrow YN$ + $\Lambda\Lambda \rightarrow \Xi N \rightarrow YN$ (NSC97f)	3.98×10^{-2}	0.49
$\Lambda\Lambda \rightarrow \Lambda\Lambda \rightarrow YN$ + $\Lambda\Lambda \rightarrow \Xi N \rightarrow YN$ (hybrid)	2.55×10^{-2}	0.13

observe that, even if it induces a small component in the wave function, this mixing can modify moderately the rate, either by increasing it in about 10% (NSC97f model) or by decreasing it in about 30% (hybrid model). A more substantial change is observed in the relative importance between the Λn and ΣN decay rates, which is inverted drastically, from a factor of 5 in the absence of the $\Lambda\Lambda$ - ΞN mixing to about 0.5 (NSC97f model) or 0.1 (hybrid model) when this new wave-function component is considered. An exclusive measurement of the decay of ${}_{\Lambda\Lambda}^6\text{He}$ hypernuclei into Λn and $\Sigma^- p$ final states would provide valuable information to confirm the importance of the strong interaction mixing effects in the decay mechanism and could possibly help in constraining some of the strong coupling constants involving a Ξ hyperon.

The complete two-body nonmesonic decay rate Γ of ${}_{\Lambda\Lambda}^6\text{He}$ contains also the processes induced by a ΛN pair and as such one may write $\Gamma = \Gamma_{\Lambda N \rightarrow NN} + \Gamma_{\Lambda\Lambda \rightarrow YN}$. The decay rate for the $\Lambda N \rightarrow NN$ channel has been computed [26] to be $\Gamma_{\Lambda N \rightarrow NN} = 0.96 \Gamma_{\Lambda} \approx 2\Gamma_{\Lambda}({}^5\text{He})$. Comparing this result to those of the $\Lambda\Lambda$ -induced mode calculated in the present work, one can see that the decay rate for the $\Lambda\Lambda \rightarrow YN$ transition with $\Lambda\Lambda$ - $\Lambda\Lambda$ diagonal correlations amounts to 3.7% of the one-nucleon-induced rate $\Gamma_{\Lambda N \rightarrow NN}$, while the inclusion of the $\Lambda\Lambda$ - ΞN mixing produces a slight increase in this percentage up to 4.1% (NSC97f model) or a decrease down to 2.6% (hybrid model).

VI. SUMMARY AND CONCLUSIONS

We have quantified the effects of the strong interaction in the decay rate of the ${}_{\Lambda\Lambda}^6\text{He}$ hypernucleus, paying special attention to the new $\Xi N \rightarrow \Lambda N$ and $\Xi N \rightarrow \Sigma N$ weak decay channels, which appear with the opening of the strongly coupled state $\Lambda\Lambda \rightarrow \Xi N$. The other unexplored weak decay channels, $\Sigma\Sigma \rightarrow \Lambda N$ and $\Sigma\Sigma \rightarrow \Sigma N$, have not been addressed in the present paper due to the comparative smallness of the $\Lambda\Lambda \rightarrow \Sigma\Sigma$ component of the initial wave function in the relevant interaction range. The new wave functions have been obtained by solving the in-medium scattering matrix (G matrix) for the interacting baryons in the initial hypernucleus. In addition, the effects of the strong interaction on the final state have been studied through the solution of the scattering matrix (T matrix), describing only the interaction between the two weakly emitted baryons. Our weak interaction model is based on the exchange of mesons belonging to the ground-state pseudoscalar and vector mesons and requires the use of flavor-SU(3) and flavor-SU(3) \times spin-SU(2) symmetry, respectively, to determine the unknown baryon-baryon-meson coupling constants.

Our work shows remarkable sensitivity of the decay mechanism to the strong interaction. In particular, the consideration of the mixing to ΞN initial states increases the $\Lambda\Lambda$ -induced decay rate by about 10% in the case of a model that employs the NSC97f strong coupling constants or decreases it by about 30% if the strong baryon-baryon-meson coupling constants involving a Ξ hyperon are derived from a chiral effective Lagrangian. The new $\Lambda\Lambda$ -induced decay rate represents about 3–4% of the dominant one-nucleon-induced rate $\Gamma_{\Lambda N \rightarrow NN}$.

Despite the small overall contribution of the $\Lambda\Lambda$ channel to the decay of ${}_{\Lambda\Lambda}^6\text{He}$, substantial changes are observed in

the $\Gamma_{\Lambda n}/(\Gamma_{\Sigma^0 n} + \Gamma_{\Sigma^- p})$ ratio when the strong interaction is carefully treated. When the mixing to ΞN states is considered in the $\Lambda\Lambda$ -correlated wave function, the relative contribution of the Λn and ΣN decay rates gets inverted with respect to what is found when only $\Lambda\Lambda$ diagonal components are considered, changing the ratio $\Gamma_{\Lambda n}/(\Gamma_{\Sigma^0 n} + \Gamma_{\Sigma^- p})$ from a value of 5 to 0.5 or 0.1, for the two abovementioned models of the strong Ξ -hyperon couplings. This sensitivity can be used experimentally to learn about the strong interaction in the strangeness $S = -2$ sector.

ACKNOWLEDGMENTS

This work is partly supported by the Spanish Ministerio de Economía y Competitividad (MINECO) under Project No. MDM-2014-0369 of ICCUB (Unidad de Excelencia María de Maeztu) and, with additional European FEDER funds under Contracts No. FIS2014-54762-P and No. FIS2017-87534-P. Support has also been received from the Generalitat de Catalunya under Contract No. 2014SGR-401 and the Secretariat for Universities and Research of the Ministry of Business and Knowledge of the Government of Catalonia, under the fellowship FI-DGR2015 2017FI_B2 00054.

APPENDIX

In this Appendix we derive the expressions of the coupling constants at the weak and strong vertices of the diagram depicted in Fig. 1, employing appropriate Lagrangians. To give the numerical estimates of the coupling constants for the pseudoscalar mesons, we use the results of an analysis that included the weak decays of the decuplet and the octet baryons. The coupling constants for the vector mesons are obtained from a model [35] based on a global fit to the octet axial currents, the strong decays of the decuplet, the s -wave weak decays of the octet, and the weak decay of the Ω^- .

1. Strong baryon-baryon-meson couplings

The description of the interaction between two baryons of the $(1/2)^+$ octet through the exchange of either a pseudoscalar or a vector meson needs the knowledge of the interaction Lagrangian connecting two baryons and a meson for each of the vertices involved in the corresponding diagram. The formalism for the construction of such Lagrangians was developed by Coleman *et al.* [36] and Callan *et al.* [37] in 1968. In these types of realizations whenever functions of the Goldstone bosons appear, they are always accompanied by at least one space-time derivative. Because the interaction with Goldstone bosons must vanish at zero momentum in the chiral limit the expansion of the Lagrangian at low energies is in powers of derivatives and pion masses.

a. Pseudoscalar mesons

The strong Lagrangian corresponding to the exchange of a pseudoscalar meson has the following form [38–40]:

$$\begin{aligned} \mathcal{L}^S = & \text{Tr}[\bar{B}(i\gamma^\mu \nabla_\mu)B] - M_B \text{Tr}[\bar{B}B] \\ & + D \text{Tr}[\bar{B}\gamma^\mu \gamma_5 \{u_\mu, B\}] \\ & + F \text{Tr}[\bar{B}\gamma^\mu \gamma_5 [u_\mu, B]], \end{aligned} \quad (\text{A1})$$

TABLE VIII. Strong pseudoscalar meson couplings to the octet baryons, where D and F are the couplings of the pseudoscalar Lagrangian of Eq. (A1) and \bar{M} denotes the average mass of the baryons at the baryon-baryon-meson vertex.

Coupling	Analytic value	$g_{BB\phi}^S$
$NN\pi$	$\frac{D+F}{2f_\pi} 2\bar{M}$	13.83
$NN\eta$	$\frac{3F-D}{2\sqrt{3}f_\pi} 2\bar{M}$	4.14
ΛNK	$-\frac{3D+F}{2\sqrt{3}f_\pi} 2\bar{M}$	-15.37
$\Lambda\Lambda\eta$	$-\frac{D}{\sqrt{3}f_\pi} 2\bar{M}$	-11.77
$\Lambda\Sigma\pi$	$\frac{D}{\sqrt{3}f_\pi} 2\bar{M}$	12.19
ΣNK	$\frac{D-F}{2f_\pi} 2\bar{M}$	3.78
$\Sigma\Sigma\pi$	$\frac{F}{f_\pi} 2\bar{M}$	13.36
$\Sigma\Sigma\eta$	$\frac{D}{\sqrt{3}f_\pi} 2\bar{M}$	12.60
$\Xi\Lambda K$	$\frac{3F-D}{2\sqrt{3}f_\pi} 2\bar{M}$	5.36
$\Xi\Sigma K$	$-\frac{D+F}{2f_\pi} 2\bar{M}$	-18.47
$\Xi\Xi\pi$	$-\frac{D-F}{\sqrt{2}f_\pi} 2\bar{M}$	-4.68
$\Xi\Xi\eta$	$-\frac{3F+D}{2\sqrt{3}f_\pi} 2\bar{M}$	-19.77

where $F = 0.52$ MeV and $D \equiv 0.85$ MeV are the octet baryon to meson couplings, $B (B_i^j = (B_i^j)^\dagger \gamma_4)$ is the matrix representing the inbound (outbound) baryons,

$$B = \begin{pmatrix} \frac{1}{\sqrt{2}}\Sigma^0 + \frac{1}{\sqrt{6}}\Lambda & \Sigma^+ & p \\ \Sigma^- & -\frac{1}{\sqrt{2}}\Sigma^0 + \frac{1}{\sqrt{6}}\Lambda & n \\ \Xi^- & \Xi^0 & -\frac{2}{\sqrt{6}}\Lambda \end{pmatrix}, \quad (\text{A2})$$

and $\nabla_\mu B = \partial_\mu B + [\Gamma_\mu, B]$ is the covariant derivative introduced to account for gauge invariance. The dependence on the meson fields is contained in the Γ_μ and u_μ operators:

$$\Gamma_\mu = \frac{1}{2}(u^\dagger \partial_\mu u + u \partial_\mu u^\dagger), \quad u_\mu = \frac{i}{2}(u \partial_\mu u^\dagger - u^\dagger \partial_\mu u), \quad (\text{A3})$$

where u is defined as $u = e^{i\frac{\phi}{\sqrt{2}f_\pi}} \simeq 1 + i\frac{1}{\sqrt{2}f_\pi}\phi$, with $f_\pi = 93$ MeV being the pion-decay constant and ϕ the self-adjoint matrix of inbound pseudoscalar mesons,

$$\phi = \begin{pmatrix} \frac{1}{\sqrt{2}}\pi^0 + \frac{1}{\sqrt{6}}\eta & \pi^+ & K^+ \\ \pi^- & -\frac{1}{\sqrt{2}}\pi^0 + \frac{1}{\sqrt{6}}\eta & K^0 \\ K^- & \bar{K}^0 & -\frac{2}{\sqrt{6}}\eta \end{pmatrix}. \quad (\text{A4})$$

The Lagrangian of Eq. (A1) allows us to derive the Yukawa-type coupling constants of the baryons to the pseudoscalar mesons displayed in Table VIII.

b. Vector mesons

The interaction between baryons and vector mesons has not been as extensively studied as the one involving pseudoscalar mesons, but one can use HLS [31], to accommodate vector mesons consistently with chiral symmetry. To incorporate these mesons in our formalism, the following Lagrangian is

used:

$$\begin{aligned} \mathcal{L}_{VBB} = & -g \{ \langle \bar{B} \gamma_\mu [V_8^\mu, B] \rangle + \langle \bar{B} \gamma_\mu B \rangle \langle V_8^\mu \rangle \\ & + \frac{1}{4M} (F \langle \bar{B} \sigma_{\mu\nu} [\partial^\mu V_8^\nu - \partial^\nu V_8^\mu, B] \rangle \\ & + D \langle \bar{B} \sigma_{\mu\nu} \{ \partial^\mu V_8^\nu - \partial^\nu V_8^\mu, B \} \rangle) \\ & + \langle \bar{B} \gamma_\mu B \rangle \langle V_0^\mu \rangle + \frac{C_0}{4M} \langle \bar{B} \sigma_{\mu\nu} V_0^{\mu\nu} B \rangle \}, \quad (\text{A5}) \end{aligned}$$

which may be obtained from the generalization of the HLS formalism in the SU(2) to the SU(3) sector. There, V_8 and V_0 are the octet and singlet terms in the vector meson matrix, respectively,

$$V_\mu = \frac{1}{2} \begin{pmatrix} \rho^0 + \omega & \sqrt{2}\rho^+ & \sqrt{2}K^{*+} \\ \sqrt{2}\rho^- & -\rho^0 + \omega & \sqrt{2}K^{*0} \\ \sqrt{2}K^{*-} & \sqrt{2}K^{*0} & \sqrt{2}\phi \end{pmatrix}_\mu, \quad (\text{A6})$$

the SU(3) D and F constants take now the values $D = 2.4$ and $F = 0.82$, and the constant C_0 is chosen to be $3F - D$, such that the ϕNN vertex is null [according to naive expectations based in the Okubo-Zweig-Iizuka rule] and the anomalous magnetic coupling of the ωNN vertex gives $\kappa_\omega \simeq 3F - D$ [41]. The baryon mass is represented by M , while g takes the form

$$g = \frac{m}{\sqrt{2}f_\pi}, \quad (\text{A7})$$

where m is the mass of the exchanged meson.

The octet and singlet matrices can be obtained by considering the mixing of the octet and singlet components of the physical ω and ϕ mesons, which under the ideal mixing assumption leads to [42]

$$\omega = \sqrt{\frac{1}{3}}\omega_8 + \sqrt{\frac{2}{3}}\omega_0, \quad (\text{A8})$$

$$\phi = -\sqrt{\frac{2}{3}}\phi_8 + \sqrt{\frac{1}{3}}\phi_0. \quad (\text{A9})$$

The Yukawa couplings involving vector mesons are displayed in Table IX.

2. Weak baryon-baryon-meson vertices: PV contribution

a. Pseudoscalar mesons

The starting point to derive the weak vertices is the heavy baryon chiral perturbation Hamiltonian introduced by Jenkins and Manohar [35,43] to account for strangeness changing amplitudes, all the while neglecting those terms in which the decuplet baryon matrices appear. Using a lowest-order chiral analysis one can only generate parity violating amplitudes, since the weak chiral Lagrangian describing parity-conserving transitions has the wrong transformation property under the combined action of the charge and parity operators [44]. The effective Lagrangian:

$$\mathcal{L} = \sqrt{2}(h_D \text{Tr}[\bar{B}[\xi^\dagger h_\xi, B]] + h_F \text{Tr}[\bar{B}[\xi^\dagger h_\xi, B]]), \quad (\text{A10})$$

is written in terms of the dimensionless constants $h_D = -1.69 \times 10^{-7}$ and $h_F = 3.26 \times 10^{-7}$, which can be fitted to

TABLE IX. Strong vector meson couplings to the octet baryons, with g , D , F , and C_0 being the couplings of the strong VBB Lagrangian of Eq. (A5).

Coupling	Analytic value	g_{BBV}^S
$NN\rho(V)$	$-\frac{1}{2}g$	2.95
$NN\rho(T)$	$-\frac{D+F}{2}g$	9.49
$NN\omega(V)$	$\frac{2\sqrt{2}+3}{2\sqrt{3}}g$	3.54
$NN\omega(T)$	$\frac{\sqrt{2}C_0+D+F}{2\sqrt{3}}g$	5.62
$\Lambda NK^*(V)$	$-\frac{\sqrt{3}}{2}g$	-5.11
$\Lambda NK^*(T)$	$-\frac{D+3F}{2\sqrt{3}}g$	-8.27
$\Lambda\Lambda\omega(V)$	$\frac{\sqrt{2}+1}{\sqrt{3}}g$	8.22
$\Lambda\Lambda\omega(T)$	$\frac{\sqrt{2}C_0+2D}{6\sqrt{3}}g$	2.77
$\Lambda\Sigma\rho(V)$	0	0
$\Lambda\Sigma\rho(T)$	$\frac{D}{\sqrt{3}}g$	8.17
$\Sigma NK^*(V)$	$-\frac{1}{2}g$	-2.95
$\Sigma NK^*(T)$	$\frac{D-F}{2}g$	4.66
$\Sigma\Sigma\rho(V)$	$-g$	-5.89
$\Sigma\Sigma\rho(T)$	$-Fg$	-4.83
$\Sigma\Sigma\omega(V)$	$\frac{\sqrt{2}+1}{\sqrt{3}}g$	8.22
$\Sigma\Sigma\omega(T)$	$\frac{\sqrt{2}C_0+2D}{2\sqrt{3}}g$	8.31
$\Xi\Lambda K^*(V)$	$-\frac{\sqrt{3}}{2}g$	5.11
$\Xi\Lambda K^*(T)$	$\frac{D-3F}{2\sqrt{3}}g$	0.10
$\Xi\Sigma K^*(V)$	$-\frac{1}{2}g$	-2.95
$\Xi\Sigma K^*(T)$	$-\frac{D+F}{2}g$	-9.49
$\Xi\Xi\rho(V)$	$\frac{1}{2}g$	2.95
$\Xi\Xi\rho(T)$	$-\frac{F-D}{2}g$	-4.66
$\Xi\Xi\omega(V)$	$\frac{2\sqrt{2}+1}{2\sqrt{3}}g$	6.51
$\Xi\Xi\omega(T)$	$\frac{D-F}{2\sqrt{3}}g$	2.69

reproduce known meson-decay amplitudes and the s -wave nonleptonic weak decays of the baryon octet members [35]. The h operator is a 3×3 matrix with a single nonzero element, $h_{23} = 1$, which accounts for strangeness variations of $|\Delta S| = 1$. The operator ξ plays a role equivalent to the one of the u operator in the strong Lagrangian defined in the previous section. The Lagrangian of Eq. (A10) allows one to find the weak PV coupling constants of the baryons to the pseudoscalar mesons displayed in Table X.

b. Vector mesons

For the weak vertices the introduction of the $SU(6)_W$ group is necessary. This group describes the product of the $SU(3)$ flavor group with the $SU(2)_W$ spin group, which is the proper group to consider when dealing with particles in motion, as the ones involved in weak decay processes [45]. In this representation the meson fields are expressed in terms of a quark-antiquark product ϕ_b^a , where the upper and lower indices refer to the spin-flavor antiquark and quark combinations,

TABLE X. Weak PV pseudoscalar meson couplings to the octet baryons.

Coupling	Analytic value	$g_{BB\phi}^{\text{PV}}$
pnK^+	$h_D + h_F$	1.57×10^{-7}
ppK^0	$h_F - h_D$	4.95×10^{-7}
nnK^0	$2h_F$	6.52×10^{-7}
$\Xi^0 n \bar{K}^0$	0	0
$\Xi^0 p K^-$	0	0
$\Xi^0 \Lambda \pi^0$	$\frac{3h_F - h_D}{2\sqrt{3}}$	3.31×10^{-7}
$\Xi^- \Lambda \pi^-$	$\frac{h_D - 3h_F}{\sqrt{6}}$	-4.68×10^{-7}
$\Xi^0 \Lambda \eta$	$\frac{h_D - 3h_F}{2}$	-5.73×10^{-7}
$\Xi^0 \Sigma^0 \pi^0$	$-\frac{h_D + h_F}{2}$	-7.84×10^{-8}
$\Xi^- \Sigma^- \pi^0$	$\frac{h_D + h_F}{\sqrt{2}}$	1.11×10^{-7}
$\Xi^- \Sigma^0 \pi^-$	$-\frac{h_D + h_F}{\sqrt{2}}$	-1.11×10^{-7}
$\Xi^0 \Sigma^0 \eta$	$\frac{\sqrt{3}(h_D + h_F)}{2}$	1.36×10^{-7}
$\Xi^- \Sigma^- \eta$	$\frac{\sqrt{3}(h_D + h_F)}{\sqrt{2}}$	1.92×10^{-7}

respectively:

$$\phi_b^a = \varepsilon q_b \bar{q}_a, \quad \text{with} \begin{cases} \varepsilon = 1 & \text{if both } a \text{ and } b \text{ are even.} \\ \varepsilon = -1 & \text{otherwise.} \end{cases} \quad (\text{A11})$$

The labels used correspond to the fundamental representation of $\text{SU}(6)_W$, and as such, both indices range from 1 to 6. The spin-up and spin-down u quarks are assigned to 1 and 2, respectively, the d quarks are assigned to 3 and 4, and the strange quarks are assigned to 5 and 6.

For the baryons one must define the symmetric tensors:

$$B^{abc} \equiv \frac{1}{6} \sum_{\text{perm } a, b, c} S^a(1) S^b(2) S^c(3), \quad (\text{A12})$$

$$B_{abc} = \bar{B}^{abc} = \frac{1}{6} \sum_{\text{perm } a, b, c} \bar{S}^a(1) \bar{S}^b(2) \bar{S}^c(3), \quad (\text{A13})$$

where the constants a , b , and c run over the same numerical values stated before. The couplings may be found by expressing the Hamiltonian in terms of the $\text{SU}(6)_W$ tensors. This Hamiltonian is the product of two currents, each belonging to the 35 representation, and using the Clebsch-Gordan series one can extract the parity-conserving and parity-violating pieces of the Hamiltonian. As discussed before, imposing the right charge conjugation and parity (CP) transformation leads to only PV contributions, which can be expressed in terms of reduced matrix elements for the product of the appropriate representations:

$$2a_T: [(\bar{B}B)_{35} \times M_{35}]_{280_a}, \quad (\text{A14})$$

$$2a_V: [(\bar{B}B)_{35} \times M_{35}]_{\bar{280}_a}, \quad (\text{A15})$$

$$b_T: [(\bar{B}B)_{405} \times M_{35}]_{280_a}, \quad (\text{A16})$$

$$b_V: [(\bar{B}B)_{405} \times M_{35}]_{\bar{280}_a}, \quad (\text{A17})$$

TABLE XI. Weak PV vector meson couplings to the octet baryons.

Coupling	Analytic value	g_{BBV}^{PV}
pnK^{*+}	$\frac{1}{9}(-b_T + 2b_V - 5c_V)$	-6.72×10^{-7}
ppK^{*0}	$\frac{1}{9}(8a_T + b_T - \frac{1}{2}b_V + c_V)$	1.38×10^{-7}
nnK^{*0}	$\frac{1}{9}(-2a_T - \frac{1}{2}b_T + b_V + c_V)$	-4.34×10^{-7}
$\Xi^0 n \bar{K}^{*0}$	0	0
$\Xi^0 p K^{*-}$	$\frac{1}{9}(b_T - 2b_V)$	2.79×10^{-7}
$\Xi^0 \Lambda \rho^0$	$\frac{\sqrt{3}}{9}(a_T + \frac{1}{4}b_T - \frac{1}{4}b_V + \frac{1}{2}c_V)$	1.31×10^{-7}
$\Xi^- \Lambda \rho^-$	$\frac{\sqrt{6}}{9}(-a_V + \frac{1}{4}b_T - \frac{1}{4}b_V + \frac{1}{2}c_V)$	2.84×10^{-7}
$\Xi^0 \Lambda \omega$	$\frac{1}{3}(\frac{1}{3}a_T + \frac{1}{4}b_T - \frac{1}{4}b_V + \frac{1}{6}c_V)$	1.69×10^{-7}
$\Xi^0 \Sigma^0 \rho^0$	$\frac{1}{9}(-5a_T - \frac{7}{4}b_T + \frac{5}{4}b_V - \frac{5}{2}c_V)$	-4.25×10^{-7}
$\Xi^- \Sigma^- \rho^0$	$-\frac{5\sqrt{2}}{18}(2a_T + c_V)$	-2.07×10^{-7}
$\Xi^- \Sigma^0 \rho^-$	$\frac{\sqrt{2}}{9}(-5a_V + \frac{1}{4}b_T - \frac{1}{4}b_V + \frac{5}{2}c_V)$	5.56×10^{-7}
$\Xi^0 \Sigma^0 \omega$	$\frac{\sqrt{3}}{27}(-5a_T - \frac{1}{4}b_T - \frac{1}{4}b_V - \frac{5}{2}c_V)$	-8.47×10^{-8}
$\Xi^- \Sigma^- \omega$	$-\frac{5\sqrt{6}}{27}(a_T + \frac{1}{2}c_V)$	-1.20×10^{-7}

$$c_V: [(\bar{B}B)_{35} \times M_{35}]_{35_a}, \quad (\text{A18})$$

with the constants a_T , a_V , b_T , b_V , and c_V related to known amplitudes [46]:

$$a_T = \frac{1}{3}a_V = \frac{3}{5}G \cos \theta_c \sin \theta_c \langle \rho^0 | V_\mu^3 | 0 \rangle \langle p | A^{\mu 3} | p \rangle, \quad (\text{A19})$$

$$b_V = -b_T = 6 \left(\frac{1}{\sqrt{3}} A_{\Lambda p} + A_{\Sigma^+ p} \right), \quad (\text{A20})$$

$$c_V = 3(\sqrt{3} A_{\Lambda p} + A_{\Sigma^+ p}). \quad (\text{A21})$$

The values $A_{\Sigma^+ p} = -3.27 \times 10^{-7}$ and $A_{\Lambda p} = 3.25 \times 10^{-7}$ obtained from data on the experimental angular distribution of the decay products and on the polarization of the final baryon [47] are used. The final general expression accounting for the weak PV baryon-baryon-vector meson couplings is

$$\begin{aligned} & a_T [\bar{B}^{ij2} B_{ij1} \bar{\phi}_3^6 - \bar{B}^{ij3} B_{ij6} \bar{\phi}_2^1 - \bar{B}^{ij1} B_{ij2} \bar{\phi}_4^5 + \bar{B}^{ij4} B_{ij5} \bar{\phi}_1^2] \\ & a_V [\bar{B}^{ij2} B_{ij5} \bar{\phi}_3^2 - \bar{B}^{ij3} B_{ij2} \bar{\phi}_2^5 - \bar{B}^{ij1} B_{ij6} \bar{\phi}_4^1 + \bar{B}^{ij4} B_{ij1} \bar{\phi}_1^6] \\ & b_T [\bar{B}^{ij2} B_{i16} \bar{\phi}_3^j - \bar{B}^{ij3} B_{i16} \bar{\phi}_2^j - \bar{B}^{23i} B_{ij6} \bar{\phi}_j^1 + \bar{B}^{23i} B_{ij1} \bar{\phi}_j^6 \\ & \quad - \bar{B}^{i1j} B_{25i} \bar{\phi}_4^j + \bar{B}^{ij4} B_{i25} \bar{\phi}_1^j + \bar{B}^{i14} B_{ij5} \bar{\phi}_j^2 - \bar{B}^{i14} B_{ij2} \bar{\phi}_j^5] \\ & b_V [\bar{B}^{ij2} B_{i25} \bar{\phi}_3^j - \bar{B}^{ij3} B_{i25} \bar{\phi}_2^j + \bar{B}^{i23} B_{ij5} \bar{\phi}_j^2 - \bar{B}^{23i} B_{ij2} \bar{\phi}_j^5 \\ & \quad - \bar{B}^{i1j} B_{16i} \bar{\phi}_4^j + \bar{B}^{ij4} B_{16i} \bar{\phi}_1^j - \bar{B}^{14i} B_{ij6} \bar{\phi}_j^1 + \bar{B}^{i14} B_{ij1} \bar{\phi}_j^6] \\ & c_V [\bar{B}^{ijk} B_{ij6} \bar{\phi}_4^k - \bar{B}^{ij4} B_{ijk} \bar{\phi}_k^6 - \bar{B}^{ijk} B_{ij5} \bar{\phi}_3^k + \bar{B}^{ij3} B_{ijk} \bar{\phi}_k^5], \end{aligned} \quad (\text{A22})$$

where the $\text{SU}(6)_W$ tensor terms must be expanded in terms of the physical fields to write down the $\langle B'M | H_{\text{PV}} | B \rangle$ elements of interest. The resulting expressions and numerical results of the weak PV coupling constants of baryons to vector mesons are shown in Table XI.

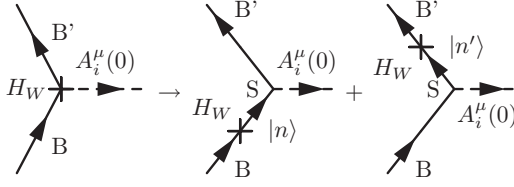


FIG. 3. Pole model diagrams contributing to the weak PC baryon-baryon-meson amplitudes. The label S denotes a strong BBM vertex.

3. Weak baryon-baryon-meson vertices: PC contribution

As stated above, the use of the weak effective Hamiltonian at lowest order allows us to obtain only the parity-violating amplitudes. The standard method to compute the parity-conserving amplitudes is based on the pole model [48], according to which the weak transition is shifted from the meson vertex to the baryonic (and mesonic) line, as represented in Fig. 3. The starting point is to consider the transition amplitude for the nonleptonic emission of a meson, $B \rightarrow B' M_i(q)$:

$$\langle B' M_i(q) | H_W | B \rangle = \int d^4x e^{iqx} \theta(x^0) \langle B' | [\partial A_i(x), H_W] | B \rangle, \quad (\text{A23})$$

where $A_i(x)$ is the axial current associated with the meson field and H_W is the weak interaction Lagrangian. Inserting a complete set of states $\sum_n |n\rangle \langle n|$ into Eq. (A23) leads to a series of contributions among which the dominant one corresponds to the baryon $(1/2)^+$ pole terms, which become singular in the SU(3) soft-meson limit and represent the leading contribution to the PC amplitudes [47]:

$$\begin{aligned} & \langle B' M_i(q) | H_W | B \rangle \\ & \sim \sum_n \left[\delta(\vec{p}_n - \vec{p}_{B'} - \vec{q}) \frac{\langle B' | A_i^\mu(0) | n \rangle \langle n | H_W(0) | B \rangle}{p_B^0 - p_n^0} \right] \\ & + \sum_{n'} \left[\delta(\vec{p}_B - \vec{p}_{n'} - \vec{q}) \frac{\langle B' | H_W(0) | n' \rangle \langle n' | A_i^\mu(0) | B \rangle}{p_B^0 - q^0 - p_{n'}^0} \right]. \end{aligned} \quad (\text{A24})$$

For the calculation of the weak pole vertices it is necessary to express the physical states in terms of the baryon octet fields $|B_i\rangle$, as well as the meson states in terms of $|M_i\rangle$ [49]. Furthermore, the mesonless weak transition between baryons, $\langle B | H_W(0) | B' \rangle$, can be computed using low-energy theorems for mesons. These theorems express the matrix element for the emission of a meson of zero (or small) four-momentum in terms of the corresponding matrix element in the absence of the soft meson and some equal-time commutators of currents [50]. They are based in the existence of certain symmetry in a given physical process, which gives rise to degenerate multiplets (a state containing an arbitrary number of Goldstone bosons) with couplings related by the symmetry. Therefore, we are able to relate the strong scattering amplitudes to the weak vertices:

$$\begin{aligned} \lim_{q \rightarrow 0} \langle B \xrightarrow{\text{PV}} B' M_i \rangle &= \lim_{q \rightarrow 0} \langle B' M_i | H_{\text{PV}} | B \rangle \\ &= -\frac{i}{f_\pi} \langle B' | [F_i, H_6] | B \rangle, \end{aligned} \quad (\text{A25})$$

where, following Cabibbo's theory, we have assumed that the weak Hamiltonian transforms like the sixth component of an octet, H_6 , according to the CP invariance of $H_W^{\Delta S=1}$, and F_i are the corresponding SU(3) generators.

To compute the last term of Eq. (A25), one can use the completely antisymmetric, f_{ijk} , and symmetric, d_{ijk} , SU(3) coefficients [51] to express the action of the F_i generator on a baryon field,

$$F_i |B_j\rangle = i f_{ijk} |B_k\rangle, \quad (\text{A26})$$

and the weak transition between baryon fields in terms of two reduced matrix elements, A and B ,

$$\langle B_k | H_6 | B_j \rangle = i A f_{6jk} + B d_{6jk}, \quad (\text{A27})$$

which can be determined by a fit to experimental data for specific PV transitions, for which we choose the $\Sigma^+ \rightarrow p + \pi^0$ (A_{Σ^+p}) and $\Lambda \rightarrow p + \pi^-$ ($A_{\Lambda p}$) processes:

$$A_{\Sigma^+p} = \frac{i}{4f_\pi} (B - A), \quad (\text{A28})$$

$$A_{\Lambda p} = -\frac{i}{f_\pi} \frac{-3A - B}{4\sqrt{3}}. \quad (\text{A29})$$

Combining these expressions, we obtain

$$-\frac{i}{f_\pi} A = A_{\Sigma^+p} - \sqrt{3} A_{\Lambda p}, \quad (\text{A30})$$

$$-\frac{i}{f_\pi} B = -\sqrt{3} A_{\Lambda p} - 3A_{\Sigma^+p}. \quad (\text{A31})$$

Therefore, when inserting the above relations in Eq. (A27), one can obtain the weak PC baryon transitions required in the pole model, $B_j \leftrightarrow B_k$, in terms of the $\Sigma^+ \rightarrow p + \pi^0$ and $\Lambda \rightarrow p + \pi^-$ PV amplitudes.

One should note that, in principle, contributions to the PC amplitudes coming from the poles in the meson propagator are also possible. These contributions have not been included, in part due to their small contribution in comparison to those of baryon poles, but also due to the uncertainty in the phase between baryon and meson pole terms.

The expressions of the weak PC coupling constants of baryons to pseudoscalar and vector mesons are shown in Tables XII and XIII, respectively. The strong coupling constants in the expressions of Table XII should be replaced by the numerical values listed in Table VIII, to obtain the weak PC couplings involving pseudoscalar mesons. Analogously the weak PC vector and tensor couplings involving vector mesons are obtained by inserting, respectively, the vector and tensor values of the strong coupling constants listed in Table IX into the expressions of Table XIII.

TABLE XII. Weak baryon-baryon-pseudoscalar meson parity-conserving couplings, $g_{BB\phi}^{\text{PC}}$.

Coupling	Analytic value
pnK^+	$g_{\Lambda\rho K^+}^S \frac{1}{m_n - m_\Lambda} \frac{-A_{\Lambda\rho}}{\sqrt{2}} + g_{\Sigma^0\rho K^+}^S \frac{1}{m_n - m_{\Sigma^0}} \frac{-A_{\Sigma+p}}{\sqrt{2}}$
ppK^0	$g_{\rho\Sigma^+\bar{K}^0}^S \frac{1}{m_p - m_{\Sigma^+}} A_{\Sigma+p}$
nnK^0	$g_{n\Lambda\bar{K}^0}^S \frac{1}{m_n - m_\Lambda} \frac{-A_{\Lambda\rho}}{\sqrt{2}} + g_{n\Sigma^0\bar{K}^0}^S \frac{1}{m_n - m_{\Sigma^0}} \frac{-A_{\Sigma+p}}{\sqrt{2}}$
$\Xi^0 n\bar{K}^0$	$g_{\Lambda n K^0}^S \frac{1}{m_{\Xi^0} - m_\Lambda} \frac{1}{\sqrt{2}} (A_{\Lambda\rho} - \sqrt{3}A_{\Sigma+p}) + g_{\Sigma^0 n K^0}^S \frac{1}{m_{\Xi^0} - m_{\Sigma^0}} \frac{-1}{2\sqrt{2}} (A_{\Sigma+p} + \sqrt{3}A_{\Lambda\rho}) + g_{\Xi^0\Lambda K^0}^S \frac{1}{m_n - m_\Lambda} \frac{-A_{\Lambda\rho}}{\sqrt{2}} + g_{\Xi^0\Sigma^0 K^0}^S \frac{1}{m_n - m_{\Sigma^0}} \frac{-A_{\Sigma+p}}{\sqrt{2}}$
$\Xi^0 pK^-$	$g_{\Lambda\rho K^+}^S \frac{1}{m_{\Xi^0} - m_\Lambda} \frac{1}{\sqrt{2}} (A_{\Lambda\rho} - \sqrt{3}A_{\Sigma+p}) + g_{\Sigma^0\rho K^+}^S \frac{1}{m_{\Xi^0} - m_{\Sigma^0}} \frac{-1}{2\sqrt{2}} (A_{\Sigma+p} + \sqrt{3}A_{\Lambda\rho}) + g_{\Xi^0\Sigma^+ K^+}^S \frac{1}{m_p - m_{\Sigma^+}} A_{\Sigma+p}$
$\Xi^0 \Lambda\pi^0$	$g_{\Xi^0\Xi^0\pi^0}^S \frac{1}{m_\Lambda - m_{\Xi^0}} \frac{1}{\sqrt{2}} (A_{\Lambda\rho} - \sqrt{3}A_{\Sigma+p}) + g_{\Lambda\Sigma^0\pi^0}^S \frac{1}{m_{\Xi^0} - m_{\Sigma^0}} \frac{-1}{2\sqrt{2}} (A_{\Sigma+p} + \sqrt{3}A_{\Lambda\rho})$
$\Xi^- \Lambda\pi^-$	$g_{\Xi^- \Lambda\pi^+}^S \frac{1}{m_{\Xi^-} - m_{\Sigma^-}} \frac{1}{2} (\sqrt{3}A_{\Lambda\rho} + A_{\Sigma+p}) + g_{\Xi^- \Xi^0\pi^+}^S \frac{1}{m_\Lambda - m_{\Xi^0}} \frac{1}{\sqrt{2}} (A_{\Lambda\rho} - \sqrt{3}A_{\Sigma+p})$
$\Xi^0 \Lambda\eta$	$(g_{\Xi^0\Xi^0\eta}^S - g_{\Lambda\Lambda\eta}^S) \frac{1}{m_\Lambda - m_{\Xi^0}} \frac{1}{\sqrt{2}} (A_{\Lambda\rho} - \sqrt{3}A_{\Sigma+p})$
$\Xi^0 \Sigma^0\pi^0$	$g_{\Xi^0\Xi^0\pi^0}^S \frac{1}{m_{\Sigma^0} - m_{\Xi^0}} \frac{-1}{2\sqrt{2}} (A_{\Sigma+p} + \sqrt{3}A_{\Lambda\rho}) + g_{\Sigma^0\Lambda\pi^0}^S \frac{1}{m_{\Xi^0} - m_\Lambda} \frac{1}{\sqrt{2}} (A_{\Lambda\rho} - \sqrt{3}A_{\Sigma+p})$
$\Xi^- \Sigma^- \pi^0$	$(g_{\Xi^- \Xi^- \pi^0}^S - g_{\Sigma^- \Sigma^- \pi^0}^S) \frac{1}{m_{\Sigma^-} - m_{\Xi^-}} \frac{1}{2} (\sqrt{3}A_{\Lambda\rho} + A_{\Sigma+p})$
$\Xi^- \Sigma^0\pi^-$	$(g_{\Sigma^- \Sigma^0\pi^+}^S \frac{1}{m_{\Xi^-} - m_{\Sigma^-}} + \frac{-1}{\sqrt{2}} g_{\Xi^- \Xi^0\pi^+}^S \frac{1}{m_{\Sigma^0} - m_{\Xi^0}}) \frac{1}{2} (\sqrt{3}A_{\Lambda\rho} + A_{\Sigma+p})$
$\Xi^0 \Sigma^0\eta$	$(g_{\Xi^0\Xi^0\eta}^S - g_{\Sigma^0\Sigma^0\eta}^S) \frac{1}{m_{\Sigma^0} - m_{\Xi^0}} \frac{-1}{2\sqrt{2}} (A_{\Sigma+p} + \sqrt{3}A_{\Lambda\rho})$
$\Xi^- \Sigma^- \eta$	$(g_{\Xi^- \Xi^- \eta}^S - g_{\Sigma^- \Sigma^- \eta}^S) \frac{1}{m_{\Sigma^-} - m_{\Xi^-}} \frac{1}{2} (\sqrt{3}A_{\Lambda\rho} + A_{\Sigma+p})$

TABLE XIII. Weak baryon-baryon-vector meson parity-conserving couplings, g_{BBV}^{PC} .

Coupling	Analytic value
pnK^{*+}	$g_{\Lambda\rho K^{*+}}^S \frac{1}{m_n - m_\Lambda} \frac{-A_{\Lambda\rho}}{\sqrt{2}} + g_{\Sigma^0\rho K^{*+}}^S \frac{1}{m_n - m_{\Sigma^0}} \frac{-A_{\Sigma+p}}{\sqrt{2}}$
ppK^{*0}	$g_{\rho\Sigma^+\bar{K}^{*0}}^S \frac{1}{m_p - m_{\Sigma^+}} A_{\Sigma+p}$
nnK^{*0}	$g_{n\Lambda\bar{K}^{*0}}^S \frac{1}{m_n - m_\Lambda} \frac{-A_{\Lambda\rho}}{\sqrt{2}} + g_{n\Sigma^0\bar{K}^{*0}}^S \frac{1}{m_n - m_{\Sigma^0}} \frac{-A_{\Sigma+p}}{\sqrt{2}}$
$\Xi^0 n\bar{K}^{*0}$	$g_{\Lambda n K^{*0}}^S \frac{1}{m_{\Xi^0} - m_\Lambda} \frac{1}{\sqrt{2}} (A_{\Lambda\rho} - \sqrt{3}A_{\Sigma+p}) + g_{\Sigma^0 n K^{*0}}^S \frac{1}{m_{\Xi^0} - m_{\Sigma^0}} \frac{-1}{2\sqrt{2}} (A_{\Sigma+p} + \sqrt{3}A_{\Lambda\rho}) + g_{\Xi^0\Lambda K^{*0}}^S \frac{1}{m_\Lambda - m_n} \frac{-A_{\Lambda\rho}}{\sqrt{2}} + g_{\Xi^0\Sigma^0 K^{*0}}^S \frac{1}{m_{\Sigma^0} - m_n} \frac{-A_{\Sigma+p}}{\sqrt{2}}$
$\Xi^0 pK^{*-}$	$g_{\Lambda\rho K^{*+}}^S \frac{1}{m_{\Xi^0} - m_\Lambda} \frac{1}{\sqrt{2}} (A_{\Lambda\rho} - \sqrt{3}A_{\Sigma+p}) + g_{\Sigma^0\rho K^{*+}}^S \frac{1}{m_{\Xi^0} - m_{\Sigma^0}} \frac{-1}{2\sqrt{2}} (A_{\Sigma+p} + \sqrt{3}A_{\Lambda\rho}) + g_{\Xi^0\Sigma^+ K^{*+}}^S \frac{1}{m_p - m_{\Sigma^+}} A_{\Sigma+p}$
$\Xi^0 \Lambda\rho^0$	$g_{\Xi^0\Xi^0\rho^0}^S \frac{1}{m_\Lambda - m_{\Xi^0}} \frac{1}{\sqrt{2}} (A_{\Lambda\rho} - \sqrt{3}A_{\Sigma+p}) + g_{\Lambda\Sigma^0\rho^0}^S \frac{1}{m_{\Xi^0} - m_{\Sigma^0}} \frac{-1}{2\sqrt{2}} (A_{\Sigma+p} + \sqrt{3}A_{\Lambda\rho})$
$\Xi^- \Lambda\rho^-$	$g_{\Xi^- \Lambda\rho^+}^S \frac{1}{m_{\Xi^-} - m_{\Sigma^-}} \frac{1}{2} (\sqrt{3}A_{\Lambda\rho} + A_{\Sigma+p}) + g_{\Xi^- \Xi^0\rho^+}^S \frac{1}{m_\Lambda - m_{\Xi^0}} \frac{1}{\sqrt{2}} (A_{\Lambda\rho} - \sqrt{3}A_{\Sigma+p})$
$\Xi^0 \Lambda\omega$	$(g_{\Xi^0\Xi^0\omega}^S - g_{\Lambda\Lambda\omega}^S) \frac{1}{m_\Lambda - m_{\Xi^0}} \frac{1}{\sqrt{2}} (A_{\Lambda\rho} - \sqrt{3}A_{\Sigma+p})$
$\Xi^0 \Sigma^0\rho^0$	$g_{\Xi^0\Xi^0\rho^0}^S \frac{1}{m_{\Sigma^0} - m_{\Xi^0}} \frac{-1}{2\sqrt{2}} (A_{\Sigma+p} + \sqrt{3}A_{\Lambda\rho}) + g_{\Sigma^0\Lambda\rho^0}^S \frac{1}{m_{\Xi^0} - m_\Lambda} \frac{1}{\sqrt{2}} (A_{\Lambda\rho} - \sqrt{3}A_{\Sigma+p})$
$\Xi^- \Sigma^- \rho^0$	$(g_{\Xi^- \Xi^- \rho^0}^S - g_{\Sigma^- \Sigma^- \rho^0}^S) \frac{1}{m_{\Sigma^-} - m_{\Xi^-}} \frac{1}{2} (\sqrt{3}A_{\Lambda\rho} + A_{\Sigma+p})$
$\Xi^- \Sigma^0\rho^-$	$(g_{\Sigma^- \Sigma^0\rho^+}^S \frac{1}{m_{\Xi^-} - m_{\Sigma^-}} + \frac{-1}{\sqrt{2}} g_{\Xi^- \Xi^0\rho^+}^S \frac{1}{m_{\Sigma^0} - m_{\Xi^0}}) \frac{1}{2} (\sqrt{3}A_{\Lambda\rho} + A_{\Sigma+p})$
$\Xi^0 \Sigma^0\omega$	$(g_{\Xi^0\Xi^0\omega}^S - g_{\Sigma^0\Sigma^0\omega}^S) \frac{1}{m_{\Sigma^0} - m_{\Xi^0}} \frac{-1}{2\sqrt{2}} (A_{\Sigma+p} + \sqrt{3}A_{\Lambda\rho})$
$\Xi^- \Sigma^- \omega$	$(g_{\Xi^- \Xi^- \omega}^S - g_{\Sigma^- \Sigma^- \omega}^S) \frac{1}{m_{\Sigma^-} - m_{\Xi^-}} \frac{1}{2} (\sqrt{3}A_{\Lambda\rho} + A_{\Sigma+p})$

- [1] S. Kanatsuki *et al.*, in *Proceedings of the 2nd International Symposium on Science at J-PARC: Unlocking the Mysteries of Life, Matter and the Universe (J-PARC 2014)*: Tsukuba, Japan, July 12–15, 2014 [*JPS Conf. Proc.* **8**, 021018 (2015)].
- [2] K. Nakazawa, Y. Endo, K. Hoshino, H. Ito, S. Kinbara, H. Kobayashi, A. Mishina, M. K. Soe, A. M. M. Theint, R. Xu, K. T. Tint, J. Yoshida, and D. H. Zhang, *Phys. Procedia* **80**, 69 (2015).
- [3] J. K. Ahn *et al.* (E373 (KEK-PS) Collaboration), *Phys. Rev. C* **88**, 014003 (2013).
- [4] K. Nakazawa *et al.*, *Prog. Theor. Exp. Phys.* **2015**, 033D02 (2015).
- [5] T. T. Sun, E. Hiyama, H. Sagawa, H. J. Schulze, and J. Meng, *Phys. Rev. C* **94**, 064319 (2016).
- [6] E. Oset and A. Ramos, *Prog. Part. Nucl. Phys.* **41**, 191 (1998).
- [7] W. M. Alberico and G. Garbarino, *Phys. Rep.* **369**, 1 (2002).
- [8] E. Botta, T. Bressani, and G. Garbarino, *Eur. Phys. J. A* **48**, 41 (2012).
- [9] S. Ajimura *et al.*, *Phys. Rev. Lett.* **80**, 3471 (1998).
- [10] O. Hashimoto *et al.*, *Phys. Rev. Lett.* **88**, 042503 (2002).
- [11] J. H. Kim *et al.*, *Phys. Rev. C* **68**, 065201 (2003).
- [12] S. Okada *et al.*, *Phys. Lett. B* **597**, 249 (2004).
- [13] M. Agnello *et al.* (FINUDA Collaboration), *Phys. Lett. B* **701**, 556 (2011).
- [14] M. Agnello *et al.* (FINUDA Collaboration), *Phys. Lett. B* **738**, 499 (2014).
- [15] E. Botta, T. Bressani, S. Bufalino, and A. Feliciello, *Riv. Nuovo Cimento* **38**, 387 (2015).
- [16] K. Sasaki, M. Izaki, and M. Oka, *Phys. Rev. C* **71**, 035502 (2005).
- [17] C. Chumillas, G. Garbarino, A. Parreno, and A. Ramos, *Phys. Lett. B* **657**, 180 (2007).
- [18] K. Itonaga, T. Motoba, T. Ueda, and T. A. Rijken, *Phys. Rev. C* **77**, 044605 (2008).
- [19] A. Perez-Obiol, A. Parreno, and B. Julia-Diaz, *Phys. Rev. C* **84**, 024606 (2011).
- [20] A. Ramos, M. J. Vicente-Vacas, and E. Oset, *Phys. Rev. C* **55**, 735 (1997); **66**, 039903(E) (2002).
- [21] W. M. Alberico, G. Garbarino, A. Parreno, and A. Ramos, *Phys. Rev. Lett.* **94**, 082501 (2005).
- [22] G. Garbarino, A. Parreno, and A. Ramos, *Phys. Rev. Lett.* **91**, 112501 (2003).
- [23] G. Garbarino, A. Parreno, and A. Ramos, *Phys. Rev. C* **69**, 054603 (2004).
- [24] E. Bauer and G. Garbarino, *Phys. Lett. B* **698**, 306 (2011).
- [25] E. Bauer, G. Garbarino, and C. A. Rodríguez Peña, *Phys. Lett. B* **766**, 144 (2017); *Phys. Rev. C* **96**, 044303 (2017).
- [26] A. Parreno, A. Ramos, and C. Bennhold, *Phys. Rev. C* **65**, 015205 (2001).
- [27] K. Sasaki, T. Inoue, and M. Oka, *Nucl. Phys. A* **726**, 349 (2003).
- [28] E. Bauer, G. Garbarino, and C. A. Rodríguez Peña, *Phys. Rev. C* **92**, 014301 (2015).
- [29] V. G. J. Stoks and T. A. Rijken, *Phys. Rev. C* **59**, 3009 (1999).
- [30] J. Caro, C. Garcia-Recio, and J. Nieves, *Nucl. Phys. A* **646**, 299 (1999).
- [31] M. Bando, T. Kugo, S. Uehara, K. Yamawaki, and T. Yanagida, *Phys. Rev. Lett.* **54**, 1215 (1985).
- [32] J.-H. Jun, *Phys. Rev. C* **63**, 044012 (2001).
- [33] A. Parreno, C. Bennhold, and B. R. Holstein, *Phys. Rev. C* **70**, 051601 (2004).
- [34] A. Pérez-Obiol, D. R. Entem, B. Juliá-Díaz, and A. Parreño, *Phys. Rev. C* **87**, 044614 (2013).
- [35] R. P. Springer, *Phys. Lett. B* **461**, 167 (1999).
- [36] S. Coleman, J. Wess, and B. Zumino, *Phys. Rev.* **177**, 2239 (1969).
- [37] C. Callan, S. Coleman, J. Wess, and B. Zumino, *Phys. Rev.* **177**, 2247 (1969).
- [38] J. Gasser and H. Leutwyler, *Ann. Phys.* **158**, 142 (1984).
- [39] J. Gasser and H. Leutwyler, *Nucl. Phys. B* **250**, 465 (1985).
- [40] J. Gasser, M. E. Sainio, and A. Svarc, *Nucl. Phys. B* **307**, 779 (1988).
- [41] K. P. Khemchandani, H. Kaneko, H. Nagahiro, and A. Hosaka, *Phys. Rev. D* **83**, 114041 (2011).
- [42] S. Okubo, *Phys. Lett.* **5**, 165 (1963).
- [43] E. E. Jenkins and A. V. Manohar, *Phys. Lett. B* **255**, 558 (1991).
- [44] R. E. Marshak, Riazuddin, and C. P. Ryan, *Theory of Weak Interactions in Particle Physics* (Wiley-Interscience, New York, 1969).
- [45] F. E. Close, *An Introduction to Quarks and Partons* (Academic, London, 1979).
- [46] B. Desplanques, J. F. Donoghue, and B. R. Holstein, *Ann. Phys.* **124**, 449 (1980).
- [47] J. F. Donoghue, E. Golowich, and B. R. Holstein, *Dynamics of the Standard Model* (Cambridge University, Cambridge, England, 1992).
- [48] J. F. Donoghue, E. Golowich, and B. R. Holstein, *Phys. Rep.* **131**, 319 (1986).
- [49] L. de la Torre, On particle mixing and hypernuclear decay, Ph.D. thesis, UMI Dissertation Information Service, 1982.
- [50] S. L. Adler and R. F. Dashen, *Current Algebras and Applications to Particle Physics* (W.A. Benjamin, Elmsford, NY, 1968).
- [51] M. Grigorescu, *Stud. Cercetari Fiz.* **36**, 3 (1984).